frontiers
in Earth Science

Oil Retention in Shales: A Review of the Mechanism, Controls and Assessment

Yue Feng[1], Xianming Xiao[1]*, Enze Wang[2], Jian Sun[1] and Ping Gao[1]

[1]School of Energy Resources, China University of Geosciences (Beijing), Beijing, China, [2]School of Earth and Space Sciences, Peking University, Beijing, China

Shale oil is a vital alternative energy source for oil and gas and has recently received an extensive attention. Characterization of the shale oil content provides an important guiding significance for resource potential evaluation, sweet spot prediction, and development of shale oil. In this paper, the mechanism, evaluation and influencing factors of oil retention in shales are reviewed. Oil is retained in shales through adsorption and swelling of kerogen, adsorption onto minerals and storage in shale pores. Quite a few methods are developed for oil content evaluation, such as three-dimensional fluorescence quantitation, two-dimensional nuclear magnetic resonance (2D NMR), solvent extraction, pyrolysis, multiple extraction-multiple pyrolysis-multiple chromatography, logging calculation, statistical regression, pyrolysis simulation experiment, and mass balance calculation. However, the limitations of these methods represent a challenge in practical applications. On this basis, the influencing factors of the oil retention are summarized from the microscale to the macroscale. The oil retention capacity is comprehensively controlled by organic matter abundance, type and maturity, mineral composition and diagenesis, oil storage space, shale thickness, and preservation conditions. Finally, oil mobility evaluation methods are introduced, mainly including the multitemperature pyrolysis, 2D NMR, and adsorption-swelling experiment, and the influencing factors of movable shale oil are briefly discussed. The aim of this paper is to deepen the understanding of shale oil evaluation and provide a basis for further research.

Keywords: shale oil, retention mechanism, evaluation method, influencing factors, movable oil

INTRODUCTION

Compared to conventional petroleum systems, shale strata exhibit the characteristics of low porosity and ultralow permeability, and shale oil and gas have received insufficient attention for a long time due to the great difficulty of exploitation (Jarvie, 2012; Chen L. et al., 2019b; Soeder and Borglum, 2019). However, in recent years, with the progress of horizontal drilling, multistage hydraulic fracturing and other engineering techniques, shale oil and gas have become resources with an appreciable development potential (Wang et al., 2015a; Kumar et al., 2017; Zou et al., 2017; Zhao et al., 2018; Chen L. et al., 2019b; Ghanizadeh et al., 2020; Chen et al., 2021). The large-scale development of shale oil in the Permian Basin, Gulf Basin and Williston Basin has provided a new perspective for oil exploration and development (Bai et al., 2020). In 2019, the proven reserves in key shale oil exploration areas in the United States reached 232.40×10^8 bbl, shale oil production yielded 22.78×10^8 bbl (US Energy Information Administration, 2021), and shale oil exploitation is
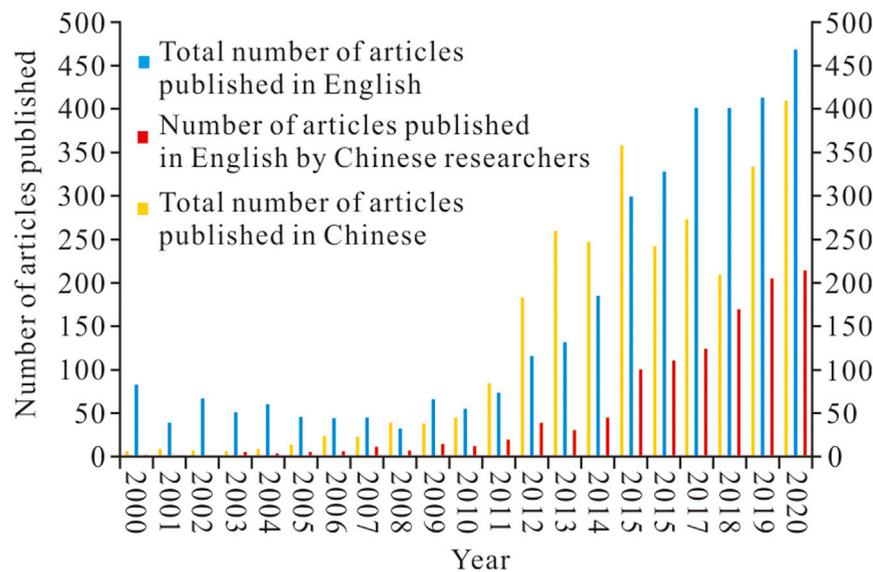
FIGURE 1 | Statistical histogram of literature on shale oil research. The data of English articles come from ScienceDirect, the blue column represents total data, the red column represents researchers from Chinese research institutions, and the data of Chinese articles (orange column) comes from CNKI. The search methods are all through title, abstract and keywords.

conducive to energy security and economic growth (Soeder and Borglum, 2020; Solarin, 2020). Russia, Argentina, Canada and other countries also possess a colossal shale oil resource potential, with recoverable shale oil resources of 746×10^8 bbl, 270×10^8 bbl, and 88×10^8 bbl, respectively (US Energy Information Administration, 2015). Inspired by the success of shale oil exploitation in the United States, these countries have launched shale oil exploration and development projects. The daily output of shale oil in Canada and Argentina is approximately 40×10^4 bbl/d and 5×10^4 bbl/d, respectively (Yang and Jin, 2019), the shale oil contained in the Mesozoic Bazhenov-Abalak Formations has been experimentally exploited in Russia, and the average horizontal well production reached 55.13 bbl/d in 2016 (Liang et al., 2019).

China contains abundant shale oil resources, the geological resources are estimated to be 27195×10^8 bbl (Yang et al., 2019), and the recoverable reserves of shale oil are 367.5×10^8 bbl (Zou et al., 2019b). With the deepening of petroleum exploration, shale oil has been found in the Ordos, Sichuan, Bohai Bay, Songliao, Junggar, Santanghu and other petroliferous basins, and notable exploration production has been documented from the Permian Lucaogou Formation in the Junggar Basin and Santanghu Basin, the Triassic Yanchang Formation in the Ordos Basin, the Cretaceous Qingshankou Formation in the Songliao Basin and the Paleogene Kongdian Formation in the Bohai Bay Basin (Wang et al., 2019a; Yang et al., 2019; Zhao W. Z. et al., 2020; Hu et al., 2020).

In recent years, an increasing number of studies on shales has been performed on their evolution of hydrocarbon generation, retention and expulsion (Shao et al., 2020; Song et al., 2021a; Sun J. et al., 2021; Hou et al., 2021b; Song et al., 2021b; Stockhausen et al., 2021), oil retention mechanism (Ritter, 2003; Tian et al., 2014; Li et al., 2016; Qiu et al., 2016; Han et al., 2017; Tian et al., 2017; Hou et al., 2020), influencing factors of shale oil enrichment

(Han et al., 2015; Zou et al., 2019a; Sun et al., 2019; Chen et al., 2020; Zhao X. Z. et al., 2020; Milliken et al., 2021) and geological evaluation (Lu et al., 2012; Kumar et al., 2017; Hu et al., 2018; Qian et al., 2018; Wang et al., 2019b; Yang and Zou, 2019; Li J. B. et al., 2020b; Wang B. Y. et al., 2021). Literatures on shale oil are increasing year by year, shale oil has become a hot topic, and Chinese scholars have carried out much shale oil research work and achieved outstanding contributions (**Figure 1**).

In contrast to conventional petroleum systems (oil migrates from source rocks to high-porosity reservoirs), shale oil is directly produced from shale strata and its associated fine-grained or organic-lean interlayers (Wang et al., 2019a). The more hydrocarbons are generated and retained, the higher the shale oil exploration potential (Wang E. Z. et al., 2021). Therefore, it is urgent to understand the oil and movable oil retained in shales. Although there have been many studies on shale oil, there is a lack of systematic investigation and summary on the mechanism of oil retention in shales and the influencing factors of oil-bearing properties.

Starting from the mechanism of shale oil retention, this paper compares various methods to quantify the total oil content in shales, summarizes its influencing factors from microcosmic to macroscopic perspectives, and then examines some available methods to estimate the movable oil in shales and discuss its influencing factors. It is anticipant that this paper could deepen the understanding of shale oil geology and provide a theoretical basis for shale oil resource evaluation and favorable exploration area prediction.

RETENTION MECHANISM OF SHALE OIL

Organic-rich shales were generally considered as source rocks in conventional petroleum systems. The relative research has

focused on the mechanism (Tissot and Welte, 1984; Huang, 1996; Kelemen et al., 2006; Zhang et al., 2006; Zhang et al., 2011; Wang et al., 2012; Liu et al., 2015; Spigolon et al., 2015; Nie et al., 2016; Burnham, 2017), characteristics, evaluation (Chen et al., 2004; Pang et al., 2005; Han et al., 2015; Hadad et al., 2017; Li J. et al., 2018; Wang et al., 2020), and influencing factors of petroleum generation and expulsion (Lewan and Stephanie, 2011; Eseme et al., 2012; Chen et al., 2014; Ma et al., 2016; Su et al., 2020; Stockhausen et al., 2021). With increasing attention given to shale oil exploration and development, research on the mechanism and influencing factors of oil retention in shales has gradually become another focus (Zou et al., 2019a; Zhao X. Z. et al., 2020; Shao et al., 2020; Hou et al., 2021b; Sun J. et al., 2021).
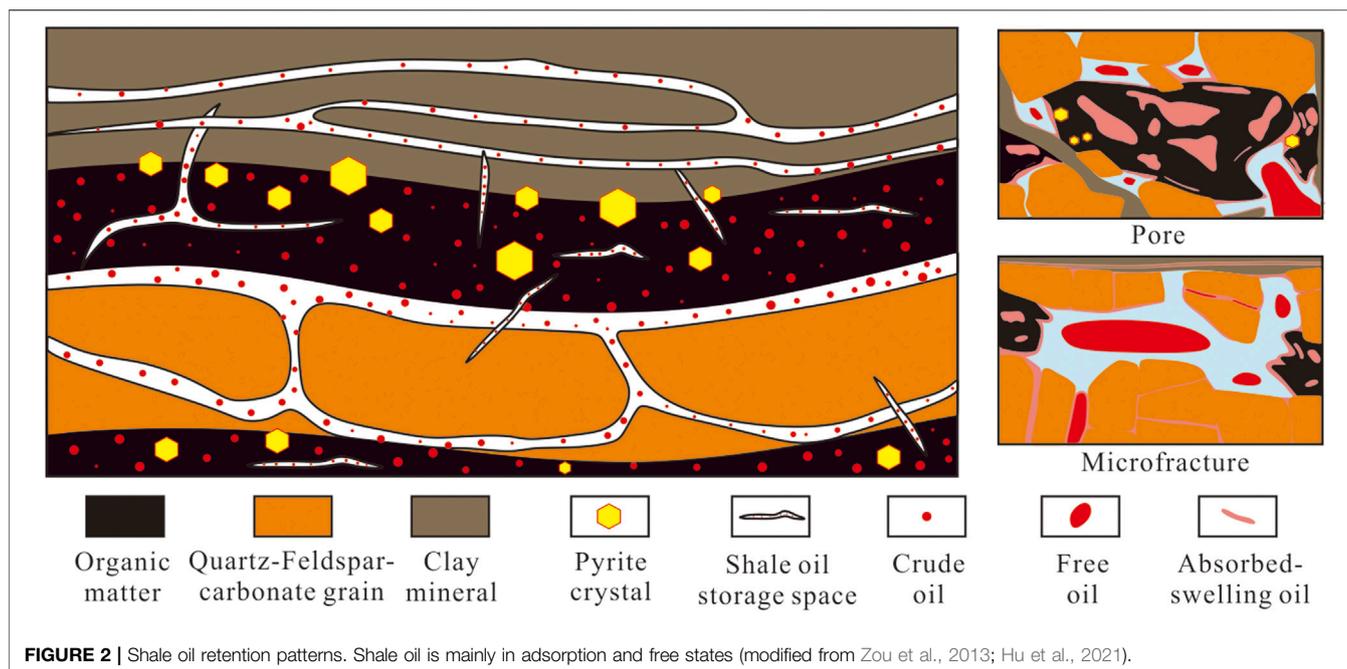
There may be a sizable capillary pressure causing oil to be drawn into and become stored in kerogen (Alfi et al., 2014). The dissolution of oil in kerogen causes kerogen volume expansion, which is similar to the swelling of organic polymers (Sandvik et al., 1992). The kerogen contained in an organic-rich shale exhibits a high cross-link density, and hydrogen bonds do not play a significant role in the intermolecular bonds of the network (Larsen and Shang, 1994; Larsen and Shang, 1997; Larsen et al., 2002; Ertas et al., 2006). The kerogen swelling behavior is controlled by the available free volume of kerogen and the size and shape of the adsorbed molecules (Stainforth, 2009). When hydrocarbon molecules are dissolved in kerogen, the interaction between the molecules and kerogen decreases, and the kerogen volume increases. Previous studies indicated that various solvents impose different swelling effects on kerogen (Larsen and Shang, 1997; Ritter, 2003). Therefore, as a multicomponent mixture, the swelling capacity of liquid petroleum depends on the contribution of each component (Pathak et al., 2017). Moreover, kerogen absorbs different components according to its preference, and oil components with similar values of Hildebrand parameter (δ) are more easily absorbed by kerogen (Ritter, 2003; Wei et al., 2012). The influence of kerogen swelling on the oil retention capacity of shales cannot be ignored. The swelling capacity of different types of kerogen varies. Tian et al. (2014) calculated that the swelling capacities of type I, II$_1$ and II$_2$ kerogens (Ro = 0.5%) are 141.7, 119.2, and 94.9 mg hydrocarbons/g TOC, respectively. Adsorption of kerogen is an important retention mode of oil (pepper, 1991), in which active kerogen provides the most active adsorption sites (Han et al., 2015). Kerogen in shale can absorb oil on the basis of satisfying the swelling effect of oil (Tian et al., 2014), with the increase of maturity, the specific surface area of kerogen gradually change and are capable of adsorbing hydrocarbons on their surface (Zhang S. J. et al., 2020). Tian et al. (2020) calculated that the adsorbed oil and the specific surface area of kerogen increased first and then decreased, the adsorbed oil content reaches its peak at Ro = 1.0%.

The shale is dominated by nanosized pore system, therefore, the interaction of fluids and pores is prominent, in other words, the influence of the adsorption of mineral particles on shale oil retention is of importance (Liu and Zhang, 2019; Wu et al., 2021). Generally, the adsorption between oil and mineral surfaces is attributed to physical interactions (such as van der Waals forces, and hydrogen bonds) or chemical interactions (Yusupova et al., 2002; Dudášová et al., 2008; Cui and Cheng, 2017; Cao et al.,

2020). According to hydrocarbon-solution adsorption tests, it is believed that the asphaltene adsorption capacity of feldspar (7.0 mg/g) is higher than that of quartz (4.5 mg/g), which is related to differences in the crystal structure and chemical composition between quartz and feldspar (Ribeiro et al., 2009). The maximum adsorption capacity of calcite for extracted shale oil-asphaltene reaches only 2.16 mg/g (Mohammadi and Sedighi, 2013), and the adsorption capacity is relatively low, which may be related to the fact that calcite (a neutral mineral) generally exhibits no electric charge (Zhang et al., 2015). Among inorganic mineral components, clay minerals provide the main adsorption surfaces for shale oil (Li et al., 2016; Ning et al., 2020). Due to the difference in cation substitution mechanism, charge and layer charge among clay minerals, the adsorption capacity of various clay minerals or even different surfaces within the same clay minerals for oil is different: 1) Al^{3+} in the montmorillonite crystal layer is replaced by divalent cations to generate a negative charge, which can attract Ca^{2+} or Na^{+}, while Si^{4+} ions in the illite crystal layer are located on the lattice surface, and the negative charge due to Al^{3+} substitution generates a greater attraction force to K^{+} so that illite can adsorb more negative organic macromolecules (Zhang et al., 2015); 2) kaolinite with an octahedral-tetrahedral structure, which is different from that of other clay minerals, contains oil-wet silicate surfaces and water-wet alumina surfaces, and the adsorption capacity of oil components per unit area is 2.47 and 1.44 mg/m^2, respectively (Tian et al., 2018). Moreover, different types of clay minerals have various specific surface areas, which may also affect adsorbed oil content (Zhu et al., 2012). However, Li et al. (2016) obtained the oil adsorption capacity of clay minerals (18 mg/g), quartz (3 mg/g) and carbonate minerals (1.8 mg/g) based on oil adsorption experiments of shale minerals. Compared to the adsorption capacity of kerogen, the oil adsorption capacity of these minerals may not be dominant in organic-rich shales. Zhao et al. (2019) reported that only 5–10% of hydrocarbons are adsorbed onto the surface of mineral particles. Considering the water-bearing capacity of shale reservoirs, the oil adsorption capacity in the water-bearing state is mainly controlled by kerogen (the remaining oil per unit of TOC is approximately 179 mg/g), which may be related to the hydrophilicity of mineral particles in shales (Wang et al., 2019b).

Nano- and micron-sized pores and microfractures are widely developed in shale oil reservoirs, constituting the reservoir space of shale oil (Zou et al., 2013; Su et al., 2018; Jin et al., 2021). The occurrence states of shale oil in pores of different scales are distinct. Free oil occurs in microfractures (Cui and Cheng, 2017; Song et al., 2020) and large pores (for example, the threshold of free oil enrichment is 30 nm, based on Liu H. M. et al. (2019), such as intergranular, intergranular and dissolution pores. The oil contained in smaller nanoscale pores coexists in the free and adsorption states (Wang et al., 2015a). With decreasing pore size, the oil in pores increasingly exhibits the adsorption state (for example, the threshold is 5 nm, based on Wang et al. (2019b)).

For a sum up from above discussion, the swelling of kerogen, adsorption of kerogen and mineral particles, and pore and fracture storage are the critical reasons for shale oil retention (**Figure 2**).

FIGURE 2 | Shale oil retention patterns. Shale oil is mainly in adsorption and free states (modified from Zou et al., 2013; Hu et al., 2021).

EVALUATION OF RETAINED OIL IN SHALES

Oil content in shales is one of the key indexes to evaluate shale oil enrichment. The characterization and evaluation of the shale oil content involve various methods, including the three-dimensional quantitative fluorescence method, two-dimensional nuclear magnetic resonance (2D NMR) method, extraction method, pyrolysis method, multiple extraction-multiple pyrolysis-multiple chromatography method, logging calculation method, statistical regression method, pyrolysis simulation experiment method and material balance method. These methods exhibit distinct characteristics (**Table 1**). The three methods of the pyrolysis, thermal simulation experiment and material balance will be futher presented, which are commonly adopted to evaluate the shale oil conten based on geochemical data.

Pyrolysis Method

The free hydrocarbon content (S_1) based on Rock-Eval pyrolysis is considered to determine the oil content in shales quickly. However, light hydrocarbon losses inevitably occur in the sampling and experimental processes (Jarvie, 2012; Jarvie, 2014). The heavy components present in kerogen, micropores and disconnected pore systems in the adsorption state can only be released at higher temperatures or when the pyrolysis temperature of organic matter is reached (Jarvie, 2012; Li M. W. et al., 2020). Zink et al. (2016) proposed that the amount of extractable S_2 component is 2.2–3.6 times the measured S_1 amount, and if this part of high-carbon number alkanes and aromatic hydrocarbons is ignored, the shale retained oil content is much underestimated. Jarvie (2012) pointed out that the oil content can be obtained according to S_1 and S_2 before and after extraction as presented in **Eq. 1**. It formed tha basis to calculate the shale oil content.

Han et al. (2015) found that the extracted S_1 (S_{1x}) component mainly comprised the extraction solvent, which suggested that the amount of shale oil should be the sum of the S_1 before and the S_2 difference before and after extraction. However, Li M. W. et al. (2018) reported that S_{1x} might be isolated hydrocarbons in nanopores, which could be regarded as part of the adsorbed hydrocarbons. In order to describe the oil content of shales more accurately, some improved pyrolysis methods have been applied (Jiang Q. G. et al., 2016; Abrams et al., 2017; Romero-Sarmiento, 2019; Gentzis et al., 2021). These oil content evaluation methods do not consider the light hydrocarbon loss attributed to sample collection and preservation and experimental operation. Cooles et al. (1986) considered that light hydrocarbons (C_{14-}) accounted for 35% of the total oil, but most of these light hydrocarbons were lost. Jiang C. Q. et al. (2016) analyzed the light hydrocarbon loss of samples *via* Rock-Eval analysis and thermal desorption-gas chromatography-mass spectrometry (TD-GC-MS)/flame ionization detection (FID) and reported that the S_1 loss for organic-rich shales could reach 15% after 360 h of open storage. Chen J. Q. et al. (2018) found that the loss rate of hydrocarbon evaporation ranged from 11 to 89% when analyzing the shale of the Middle Permian Lucaogou Formation in the Jimusar Sag. Therefore, it is necessary to correct the light hydrocarbon loss for the accurate evaluation of the shale oil content (Beti et al., 2020). Based on light hydrocarbon loss correction, Abrams et al. (2017) added a S_1 loss term (**Eq. 2**) to the original oil content equation.

With increasing maturity, the light components in shales that are easily lost in the process of core preservation and experimental analysis, and the light hydrocarbon loss exhibits an increasing dynamic trend (Zhu et al., 2015; Li J. B. et al., 2020b). Based on the above reasons, according to the difference in pyrolytic hydrocarbons between sealed freezing treatment and conventional preservation treatment (Zhu et al., 2015), newly proposed oil formation volume factor (FVF) (Chen Z. H.
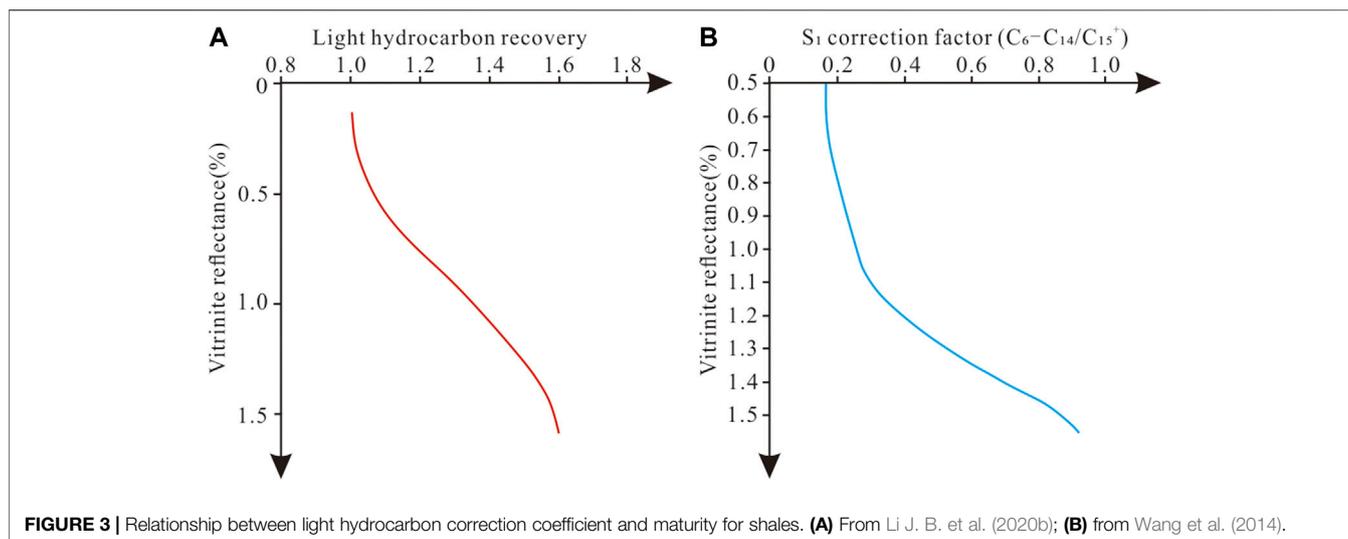
TABLE 1 | An overview of determination of retained oil content in shales.

Method	Operation step		Parameter	Characteristics	Reference
Three-dimensional quantitative fluorescence method	Shale particles with a mass of M (g) are placed in a solvent with a volume of V (L). The immersion solution is collected and detected *via* quantitative three-dimensional fluorescence. The fluorescence oil concentration C (mg/L) can be converted into the fluorescence oil content C_o (mg/g)		$C_o = C \times V_{solvent}/M$	The method is fast and efficient, but the experimental results are affected by the particle size, extraction time, ultrasound assistance and calibration curve	Liu B. et al. (2019); Qian et al. (2020)
Two-dimensional nuclear magnetic resonance (2D NMR) method	2D NMR experiments are carried out on shale samples		The total amount of ^1H compounds multiplied by the percentage of the adsorbed oil and free oil signals in the total signal	The oil and free oil contents can be determined, but the boundaries of the different fluid distribution intervals are difficult to define	Bai et al. (2019); Li J. B. et al. (2020a)
Extraction method	Chloroform extraction method	An amount M (g) of shale is heated and extracted with chloroform, and the extract is concentrated. The content of chloroform bitumen A is calculated according to the weight M_1 (g) of the weighing bottle and the weight M_2 (g) of chloroform asphalt. Correction coefficient K_a is calculated according to the light hydrocarbon (C_6-C_{14}) content in chloroform bitumen A (K_1, %), the light hydrocarbon content in alkanes of crude oil (K_2, %), and the alkane content in chloroform bitumen A (sat, %)	Total oil = chloroform bitumen A $\times K_a$ = chloroform bitumen A $\times (1 + K_1)$ = chloroform bitumen A $\times [1 + (sat \times K_2)]$	The experimental results are easy to obtain, but there is a severe loss of light hydrocarbons (C_6-C_{14}) in the process of sample preparation and solvent evaporation. The correct result of C_{14-} light hydrocarbons depends on the matching between the components of crude oil and chloroform bitumen A and the thermal maturity of the samples	Zhu et al. (2015)
	Sequential extraction method	Shale samples are extracted with different polar solvent systems, including weak polar solvents, strong polar solvents or highly polar solvents	Total oil = cumulative amount of solvent extraction (mg/g rock)	The content of shale oil in different occurrence states can be determined. Sequential extraction does not completely separate soluble organic matter with different occurrence states, and the change in solvent and extraction mode may cause a change in experimental data	Qian et al. (2017); Zhang H. et al. (2020)
Pyrolysis method	Rock-Eval pyrolysis method	The amount of thermovaporized free hydrocarbons (S_1, mg hydrocarbons/g rock) can be obtained by heating shale samples in an open pyrolysis system	Total oil = S_1	The experimental results are easy to obtain, but there are light and heavy hydrocarbon losses	Behar et al. (2001); Lu et al. (2012)
	Single routine Rock-Eval experiment	The temperature threshold (T_{OK}) is determined by the cumulative amplitude of shale and solvent-extracted shale, and cracking hydrocarbons (S_{2K}) and heavy hydrocarbons (S_{2oil}) are then rapidly separated	Total oil = $S_1 + S_{2oil}$	Conventional pyrolysis data sets can be employed to directly calculate the total oil production based on the temperature threshold, but the light hydrocarbon loss should be considered	Li J. B. et al. (2019)
	Multistep on-column thermal extraction method	Shale samples can be analyzed in a multi-step thermal extraction system to obtain a high-resolution thermal extraction curve, and the thermal peak areas can be analyzed to evaluate the oil content	Total oil = total multistep thermal extraction system (MiSTE) $\sum(P200°C + P250°C + P300°C + P350°C)$	The experimental method is inexpensive, fast and efficient, and it can measure the oil in place. However, the evaluation results should be corrected for light hydrocarbons	Abrams et al. (2017)

(Continued on following page)

TABLE 1 | (Continued) An overview of determination of retained oil content in shales.

Method	Operation step		Parameter	Characteristics	Reference
	Multistep pyrolysis method	The component contents in the different temperature ranges are obtained via programmed step-by-step pyrolysis experiment	Total oil = pyrolytic hydrocarbon peaks of nonkerogen cracking	The method is easy to operate, but it is difficult to determine the heat release temperature limit of hydrocarbons in different occurrence states in shale, and it is necessary to recover the loss of light hydrocarbons	Jiang Q. G. et al. (2016); Romero-Sarmiento (2019); Ghanizadeh et al. (2020); Gentzis et al. (2021)
Multiple extraction-multiple pyrolysis-multiple chromatographic analysis method	The total oil in shale is calculated through low-temperature immersion of cores, multiple extractions (dichloromethane and chloroform solutions), multiple pyrolysis steps, and multiple chromatographic analyses		Total oil = WO1 (amount of C_5–C_7) + WO2 (amount of C_{6+} and weight of the residual evaporation solution) + WO3 (amount of dichloromethane extraction) + WO4 (amount of chloroform extraction) + WO5 (hydrocarbons retained in shale after chloroform extraction)	The operation steps and process of this method are complex, but the loss of hydrocarbons is fully considered in this experimental method, and the analysis result is reliable	Hou et al. (2021a)
Logging calculation method	Based on logging data of the resistivity and porosity, a variable-coefficient ΔlogR model is applied to calculate the oil content		$S_1 = a \times \Delta logR_{S1} + b$ Chloroform bitumen A = $c \times \Delta logR_A + d$ (a, b, c and d are fitting coefficients of the equation)	The data for this method are easy to obtain, and the model is easy to apply and can obtain continuous oil content analysis data. However, the influence of the data quality on logging model predictions cannot be ignored. The calculation results must be corrected for light hydrocarbons and/or heavy hydrocarbons	Liu et al. (2014); Li J. B. et al. (2020b)
	With the use of NMR logging and the factor analysis method, oil saturation index (OSI) and S1 are estimated by using the bin porosity (33 ≤ $T_{2cutoff}$ < 80) corresponding to hydrocarbon production		$S_{1NMR} = (120 \times bp6 + 100) \times TOC/100$	Continuous oil content analysis data can be obtained, but the signals of the different fluids overlap, and the prediction results may contain errors	Piedrahita and Roberto (2017)
Statistical regression method	A regression statistical model can be established according to the relationship between oil retention and TOC, mineral composition and other control factors		$S_1^{cal} = 0.320 \times TOC + 0.062 \times quartz -0.007$ (for the second interval)	There may exist collinearity among the control factors, which leads to distortion of the regression model	Han et al. (2015)
Thermal simulation experiment method	Shale samples are tested via thermal simulations		The oil content in shale samples is determined corresponding to different temperature points	The experimental results are intuitive, but the experimental conditions (whether water occurs, open vs. closed vs. semiopen systems, and sample conditions) exert an impact on the results	Peng et al. (2018); Shao et al. (2020)
Material balance method	The principle of carbon mass (component) conservation is applied to determine the retained oil content		Total oil = hydrocarbon generation quantity-hydrocarbon expulsion quantity	The method is easy to calculate, but its accuracy depends on the satisfaction of certain assumptions and the quality of data	Pang et al. (2005); Wang E. Z. et al. (2021)

FIGURE 3 | Relationship between light hydrocarbon correction coefficient and maturity for shales. **(A)** From Li J. B. et al. (2020b); **(B)** from Wang et al. (2014).

et al., 2019; Li M. W. et al., 2020), and hydrocarbon generation kinetics calculations (Wang et al., 2014) consider the recovery method of S_{1loss} at different maturities, the recovery coefficient of light hydrocarbon loss becomes larger as the maturity increases (**Figure 3**), which means the light hydrocarbon calibration is necessary in the mature and high-mature stage of shale.

$$\text{Total oil} = (S_{1\,\text{whole rock}} - S_{1\,\text{extracted rock}})$$
$$+ (S_{2\,\text{whole rock}} - S_{2\,\text{extracted rock}}) \tag{1}$$

$$\text{Total oil} = (S_{1\,\text{whole rock}} - S_{1\,\text{extracted rock}})$$
$$+ (S_{2\,\text{whole rock}} - S_{2\,\text{extracted rock}}) + S_{1\,\text{loss}} \tag{2}$$

Material Balance Method

The mass of organic matter in shales that can be converted into petroleum should be constant during thermal evolution if there is not material exchange with the external environment. According to this idea, Pang et al. (2005) proposed the hydrocarbon generation potential method of rock pyrolysis, which is a statistical method based on the principle of mass balance, to calculate the hydrocarbon generation, retention and expulsion of shales. For a specific shale sample, its hydrocarbon generation potential index ($Q_g = 100 \times (S_1+S_2)/\text{TOC}$) should remain unchanged. The only reason for its change is hydrocarbon expulsion. Hence, the difference between hydrocarbon generation and expulsion is the amount of retained hydrocarbons in the shale (**Figure 4A**). However, this method does not consider the data error caused by light hydrocarbon evaporation (Chen J. Q. et al., 2018), and does not provide a clear limit on the recovery coefficient of the hydrocarbon generation potential.

Chen and Jiang (2016) statistically fitted an empirical model of the hydrocarbon index (HI) and T_{max} based on the measured data of shale samples (**Eq. 3**), converted this empirical relationship into the hydrocarbon conversion rate (Tr) (**Eq. 4**) and further clarified the hydrocarbon expulsion efficiency (**Eq. 5**). On this basis, Wang et al. (2020) thought that S_1 could be regarded as being wholly derived from S_2 *via* transformation, so the original hydrogen index (H_I^0) was selected to define the maximum value of the hydrocarbon generation capacity

of the different types of kerogen, and the hydrocarbon generation, retention and expulsion processes of shales were characterized, then the shale oil resource potential can be evaluated by the hydrocarbon retention potential (Q_r) (mg HC/g TOC) (**Figure 4B**).

In the above previous methods, the determination of the hydrocarbon expulsion threshold depends on the inflection point of the hydrocarbon generation potential index, and the determination of the hydrocarbon expulsion threshold may not be accurate. Li C. R. et al. (2020) adopted a hydrocarbon generation statistical model to simulate the changes in the hydrogen index and Q_g during the evolution of shales and proposed a quantifiable hydrocarbon expulsion efficiency (Er) (**Eq. 6**), and shale oil resources can be calculated by the difference between Tr and Er, which was applied to the Qingshankou Formation in the Songliao Basin and achieved a reasonable result (**Figure 4C**).

$$H_I = H_I^0 \left[1 - exp\left\{ -\left(\frac{T_{max}}{\beta} \right)^{\theta} \right\} \right] + c \tag{3}$$

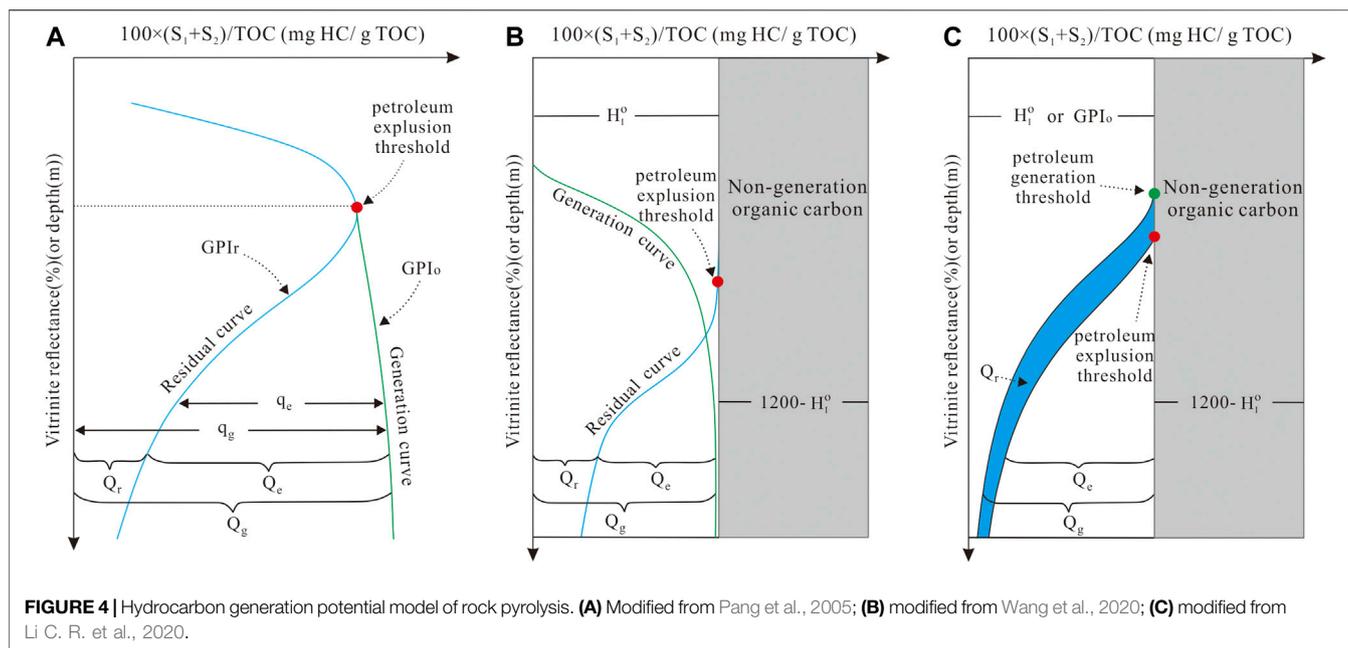$$T_r = \frac{(1000/\alpha) \times (H_I^0 - H_I)}{H_I^0 \left((1000/\alpha) - H_I \right)} \tag{4}$$

$$E_r = 1 - \frac{s_1 \times (1 - T_r)}{s_2 T_r} \tag{5}$$

$$E_r = \frac{(1000/\alpha) \times (Q_{go} - Q_g)}{Q_{go} \times \left((1000/\alpha) - Q_g \right)} \tag{6}$$

where β and θ are variables related to the type of kerogen, c is the error correction factor, α is the weight fraction of carbon relative to the generated hydrocarbons, its average value is considered to be 83.3%, $Q_{go}(\text{GPI}_o)$ represents the original hydrocarbon generation potential index.

Thermal Simulation Method

Because it is challenging to collect shale sample from immature to overmature stages, the hydrocarbon generation, retention and expulsion evolution profiles of shales can be established through thermal simulation experiments (Ma et al., 2018). Thermal

FIGURE 4 | Hydrocarbon generation potential model of rock pyrolysis. **(A)** Modified from Pang et al., 2005; **(B)** modified from Wang et al., 2020; **(C)** modified from Li C. R. et al., 2020.

simulation systems can be divided into open, closed and semiclosed systems, and they produce different results (Ghanizadeh et al., 2020). Under geological conditions, petroleum generation, retention and expulsion follow a kinetic evolution process. In a semiclosed system, thermal simulation products are allowed to be discharged during generation, which may be more suitable for uses of geological evaluation (Li J. et al., 2018; Ma et al., 2018; Zhang D. W. et al., 2020).

Thermal simulation results cannot be directly applied to the geological evaluation and prediction. According to simulation experimental data on hydrocarbon generation in low-maturity shales, kinetic parameters such as activation energy (Ea) and frequency factor (A) can be obtained, and the hydrocarbon generation, retention and expulsion characteristics of shales under geological conditions can be obtained *via* extrapolation of these parameters. A series of kinetic models of hydrocarbon generation, such as the overall reaction model, series reaction model and parallel reaction model, have been proposed. Wang et al. (2011) compared different kinetic models and considered that the discretely distributed parallel first-order kinetic model might be the most suitable model to describe the hydrocarbon generation process. At present, it is widely accepted that the thermal decomposition process of kerogen is similar to a series of independent parallel first-order chemical reactions (Wang et al., 2011; Chen et al., 2017). Although Stainforth (2009) suggested that the assumption of independent first-order reactions may be too simplistic, the prediction of a hydrocarbon generation kinetics model controlled by first-order chemical kinetics seems to be supported by actual maturity measurements (Peters et al., 2018). The vitrinite reflectance corresponding to different temperatures can be calculated with Easy%Ro (Sweeney and Burnham, 1990), PresRo™ (Carr, 1999), Pa%Ro (Xiao et al., 2005), Basin%Ro (Nielsen et al., 2017) and Easy%RoDL (Peters et al., 2018) at various heating temperature and duration, combined with thermal simulation results, to determine the oil generation, retention and expulsion characteristics of shales at different maturation stages.

INFLUENCING FACTORS OF OIL RETENTION IN SHALES

Shale oil is the oil remaining in shales during oil generation and expulsion, which is influenced by various factors. To explore the influencing factors more clearly, we examines the influencing factors of oil retention from the microscale to the macroscale. Microscopically, the oil retention in TOC per unit weight is chosen as the subject, and the influence of the organic matter type and thermal maturity on the shale oil content is investigated. Semimicroscopically, the research object is the oil retention in unit rock weight and micron-to-centimeter-scale deposition structure, and the effects of organic matter abundance, pore development and rock mineral composition on oil retention are compared. Macroscopically, the shale section is selected as the research object, and the influence of the shale thickness and preservation conditions on shale oil retention and resource evaluation is clarified.

Restriction of Organic Matter Properties on Oil Retention

Shales with oil potential mainly contains sapropelic organic matter, with a kerogen type of I or II, which exhibit a high effective organic carbon ratio and good oil generation potential (Chen and Jiang, 2015; Ma et al., 2018; Li M. W. et al., 2019b; Zou et al., 2019b; Zhao W. Z. et al., 2021). The kerogen type in shales exerts apparent control over their oil-bearing properties. Generally, type I kerogen retained more oil than type II kerogen (Bai et al., 2017; He et al., 2019). Sun J. et al. (2021), also vertified that the retained content of shales exhibits growing trend with the increase of their original HI within the "oil window" stage through thermal simulation experiments. However, some
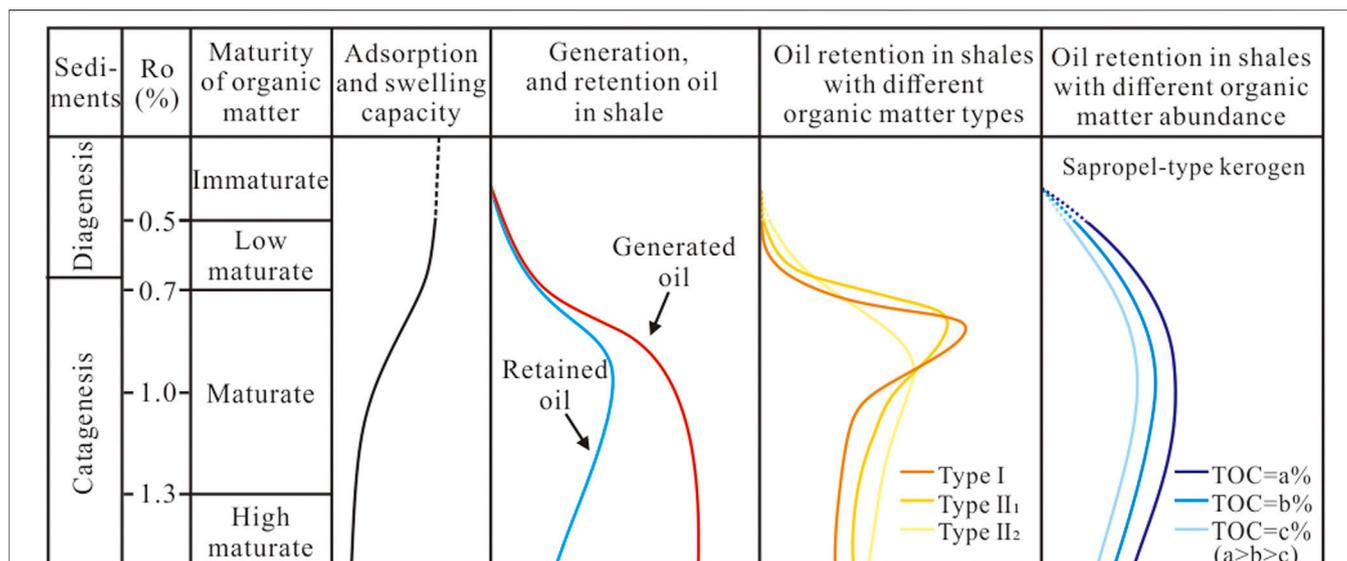
FIGURE 5 | Retention pattern of shale oil under different influence factors (modified from Tian et al., 2014; Li J. et al., 2015; Li J. et al., 2018; Yang and Zou, 2019; Zhao X. Z. et al., 2020).
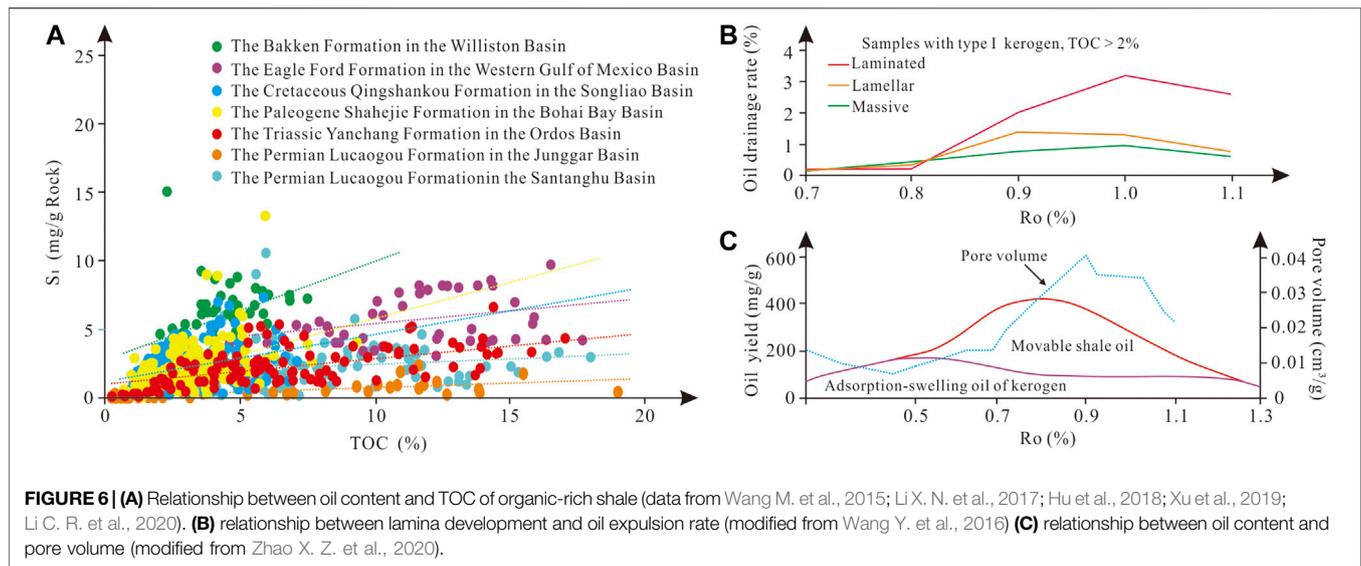
geological observations indicate that shales containing type II kerogen may contain more considerable shale oil resources compared to shales with type I kerogen (Li J. J. et al., 2015; Hu et al., 2018). This may occur because the better the type of organic matter is, the greater the hydrocarbon expulsion amount per unit of organic carbon (Chen et al., 2014; Huang et al., 2017; Ma et al., 2018; Sun J. et al., 2021), resulting in a lower retainded oil content. Tian et al. (2014) analyzed shales in the Qingshankou Formation in the northern Songliao Basin and reported that for Ro > 0.9%, the oil content per unit mass of TOC of type II kerogen is higher than that of type I kerogen, which seems to be related to the faster reduction in volume of type I kerogen per unit mass of TOC (**Figure 5**). In addition, a shale containing type II kerogen exhibits a high oxygen content, which facilitates the formation of organic acids, and the hydrocarbon expulsion efficiency is lower than that of a shale containing type I kerogen, thereby its shale oil content is higher (Li J. J. et al., 2015).

The oil content in shales is relatively low at the immature stage. Nevertheless, if the thermal maturity is too high, this leads to the so-called secondary cracking of oil into gas in shales, and oil is not effectively retained (Zhang P. Y. et al., 2021). Exploration practices of shale oil revealed that the Ro value in the shale oil palys broadly ranges from 0.5 to 1.6% (Cardott, 2012; Zhao W. Z. et al., 2020). Maturity affects the shale oil content based on the amount of oil generated and affects the hydrocarbon expulsion ability according to the composition of evolution products. With increasing thermal maturation, the density and viscosity of oil generally decrease, which encourages the flow and expulsion of oil (Wang et al., 2019b; Zhao W. Z. et al, 2021). The adsorption-swelling oil amount per unit of organic carbon is negatively correlated with increasing thermal maturity (Zhao X. Z. et al., 2021). When the oil storage space remains fixed, this inevitably

leads to the expulsion of oil. Moreover, Panahi et al. (2019) proposed that the formation, opening of hydrocarbon expulsion microfractures and fluid expulsion rate are related to thermal maturity levels based on experiments. Therefore, a moderate degree of thermal evolution is conducive to shale oil enrichment. Yang and Zou (2019) pointed out that the amount of retained oil in shales with Ro values between 0.9 and 1.3% reaches a maximum (**Figure 5**).

Control of TOC Content, Oil Storage Space and Mineral Composition on Oil Retention

Organic matter enrichment constitutes the basis of shale oil accumulation, and shales with a certain shale oil potential often exhibit a higher TOC content (Zou et al., 2013). When the type and maturity of organic matter are fixed, the TOC content determines the oil generation capacity of shales (Ma et al., 2018). Although a high TOC content suggests an increase in hydrocarbon expulsion efficiency (Sun J. et al., 2021), analysis data from shale oil plays and thermal simulation revealed that the TOC content is usually positively correlated with the shale oil content (**Figure 5**) (Li J. et al., 2015; Han et al., 2015). Hou et al. (2020) noted that shales with a high TOC content still yield a notable advantage in oil retention due to their high oil generation efficiency. An increase in TOC content also increases the content of adsorbed oil (Cao et al., 2017; Wang et al., 2019b). In addition, studies have demonstrated that a higher TOC content indicates that more organic acids are produced during the hydrocarbon generation process, which facilitates the development of dissolution pores and recrystallized intergranular pores (Liang et al., 2017; Hu et al., 2019) and provides essential oil storage spaces (Zhang et al., 2016). Therefore, an increase in organic matter abundance is conducive to shale oil enrichment. As shown

FIGURE 6 | (A) Relationship between oil content and TOC of organic-rich shale (data from Wang M. et al., 2015; Li X. N. et al., 2017; Hu et al., 2018; Xu et al., 2019; Li C. R. et al., 2020). **(B)** relationship between lamina development and oil expulsion rate (modified from Wang Y. et al., 2016) **(C)** relationship between oil content and pore volume (modified from Zhao X. Z. et al., 2020).

in **Figure 6A**, the oil content per unit mass of rock becomes larger as the organic matter abundance increases.

Shales comprise terrigenous detritus, clay minerals, carbonate, pyrite and other inorganic minerals and organic matter (Chen L. et al., 2019a). Inorganic components (clay minerals, pyrite, etc.) affect the shale oil content through oil generation and retention capacity. Clay minerals can influence the hydrocarbon generation process and mechanism through a carbon ion mechanism and/or participate in the desorption and hydrogenation/decarboxylation of solid acids (Du et al., 2021; Song et al., 2021a). Transition group elements such as Fe, Co and V in shales impose a catalytic effect on organic matter hydrocarbon generation, which can generate more oil and gas in organic-rich shales at the early burial stage (Xi et al., 2020). Studies have shown that local cementation can reduce the discharge of shale oil *via* compaction inhibition, and carbonate minerals can react with organic acids to increase oil storage spaces (Hu et al., 2019; Milliken et al., 2021). Although the wettability of shale surfaces exhibits mixed characteristics (Gao et al., 2019), clay minerals still provide considerable oil adsorption surfaces, and the increase in the clay mineral content is beneficial to the increase in oil content to a certain extent (Li Z., 2020). Furthermore, laminae are widely developed sedimentary structures in shales, representing the directional arrangement of organic matter or inorganic minerals. Shales containing laminae exhibit a high hydrocarbon generation ability, and shales containing fine laminae formed *via* biochemical deposition exhibit a more pronounced hydrocarbon generation ability (Zeng et al., 2017; Su et al., 2019). The interbedding of micron-to centimeter-scale laminae composed of different components reflects the microscale source-reservoir configuration of shales (Han et al., 2021; Liu B. et al., 2021). Shales with well-developed laminae often attain a higher oil expulsion efficiency (Wang Y. et al., 2016; Du et al., 2019) (**Figure 6B**). A considerable amount of oil migrates into feldspar-quartz laminae or carbonate laminae at the semi-to microscale after meeting the oil retention

requirements of organic-rich laminae, resulting in relatively high oil-bearing properties (Xi et al., 2020; Han et al., 2021).

Oil is adsorbed onto kerogen and mineral particles and occurs in pores and fractures in shales. The development of shale pores exerts an important control on the oil content (Li J. J. et al., 2018; Zhao X. Z. et al., 2020) (**Figure 6C**). Chen G. H. et al. (2018) reported that 80% of shale oil is distributed in macropores. In fact, with increasing pore size, pore volume and porosity, the oil content in shales usually increases (Wang et al., 2019b; Song et al., 2020; Wang B. Y. et al., 2021). Because the density of the generated oil and gas is lighter than that of kerogen, the volume expansion and the overpressure phenomenon occurs in shales, resulting in the generation of oil expulsion fractures (Sun L. D. et al., 2021). Although shale microfractures form effective oil migration channels and oil storage spaces, when the scale of microfractures reaches a certain extent, this may reduce the shale oil content. Liu B. et al. (2021) pointed out that a higher fracture density resulted in a vertical migration of shale oil, which does not promote shale oil enrichment. Zhao X. Z. et al. (2020) indicated that natural fracture development limited to the shale interior is relatively favorable to the seepage and preservation of retained oil in shales.

Influences of Shale Thickness and Preservation Conditions on Oil Retention

The thickness of organic-rich shales macroscopically controls the shale oil content. A thick shale, especially at its center part, does not facilitate oil expulsion (Leythaeuser et al., 1984). It seems that there is an effective petroleum expulsion thickness in geological conditions, and the shale beyond the thickness would have a weak oil expulsion (Jiang et al., 1986; Wang et al., 2005; Hou et al., 2017). Based on the pyrolysis experiment and geological model, Hou et al. (2017) found that the increase of the shale thickness during the oil generation stage would significantly reduce the oil expulsion efficiency. The thinner a single shale seam in a shale-

sandstone interbedding stratum, the more frequent the shale-sandstone configuration and the lower the retention of oil in the shale (Fan and Shi, 2019), while the oil-bearing properties of the interlayers (i.e., the sandstone seams) within the shale seams are improved (Raji et al., 2015). Exploration practices have verified that fault systems impart complementary control effects on both conventional and shale reservoirs, the retained oil in the shale may migrate to the shallow layers along the faults remaining active, which is unfavorable for shale oil enrichment (Fu et al., 2020; Liu B. et al., 2021). However, thick shales are not easily broken through (Fu et al., 2018). Microfractures extending only in the interior of a shale increase the shale oil storage space and fluidity, which is more benefit to shale oil enrichment (Zhao X. Z. et al., 2020). Therefore, the shale thickness plays a positive role in the oil-bearing capacity (Fan and Shi, 2019; Zhao W. Z. et al., 2021).

Preservation conditions are also important for shale oil enrichment. Lin et al. (2020) calculated that the decisive tectonic action in the Miquan area of the Junggar Basin caused a loss of 78.9% of the original shale oil resources. A relatively stable tectonic environment and high-quality top and bottom seal layers of a shale seam play positive roles in the preservation of shale oil (Liu et al., 2018; Li M. W. et al., 2019b; Liu B. et al., 2021).

EVALUATION AND INFLUCEING FACTORS OF MOVABLE OIL IN SHALES

The movable oil content in shales is the key to a high yield of shale oil (Jarvie, 2012; Li J. Q. et al., 2018; Li M. W. et al., 2019a; Li H. et al., 2020; Hu et al., 2021). It is highly important to determine the amount of movable oil and its influencing factors for shale oil prediction. This section mainly introduces three feasible and realistic methods to evaluate the shale movable oil content, including the pyrolysis, 2D NMR and adsorption-swelling calculation methods. In addition, the influencing factors of movable oil in shales are also discussed.

Evaluation of Movable Oil
Pyrolysis Method
According to available empirical data of shale oil production, Jarvie (2012) proposed the oil crossover effect, i.e., OSI > 100 mg hydrocarbons/g TOC as the indicator of movable oil in shales (**Figure 7A**). Quite a few authors have applied this standard to evaluate movable shale oil because it eliminates the influence of organic matter adsorption (Wang M. et al., 2015; Cao et al., 2017; Hu et al., 2018; Zhao X. Z. et al., 2020). Zhao X. Z. et al. (2020) indicated that the movable oil content is equal to the difference between the amount of retained oil and the oil crossover effect value (**Figure 7B**). However, the OSI method may not be fully applicable in lacustrine shales (Xue et al., 2015; Huang et al., 2020), and the OSI value and oil crossover effect dynamically change with the maturity. With increasing maturity, the OSI values gradually increase until a maximum retention capacity is reached, and then a subsequent decrease is show (**Figure 7C**) (Han et al., 2017).
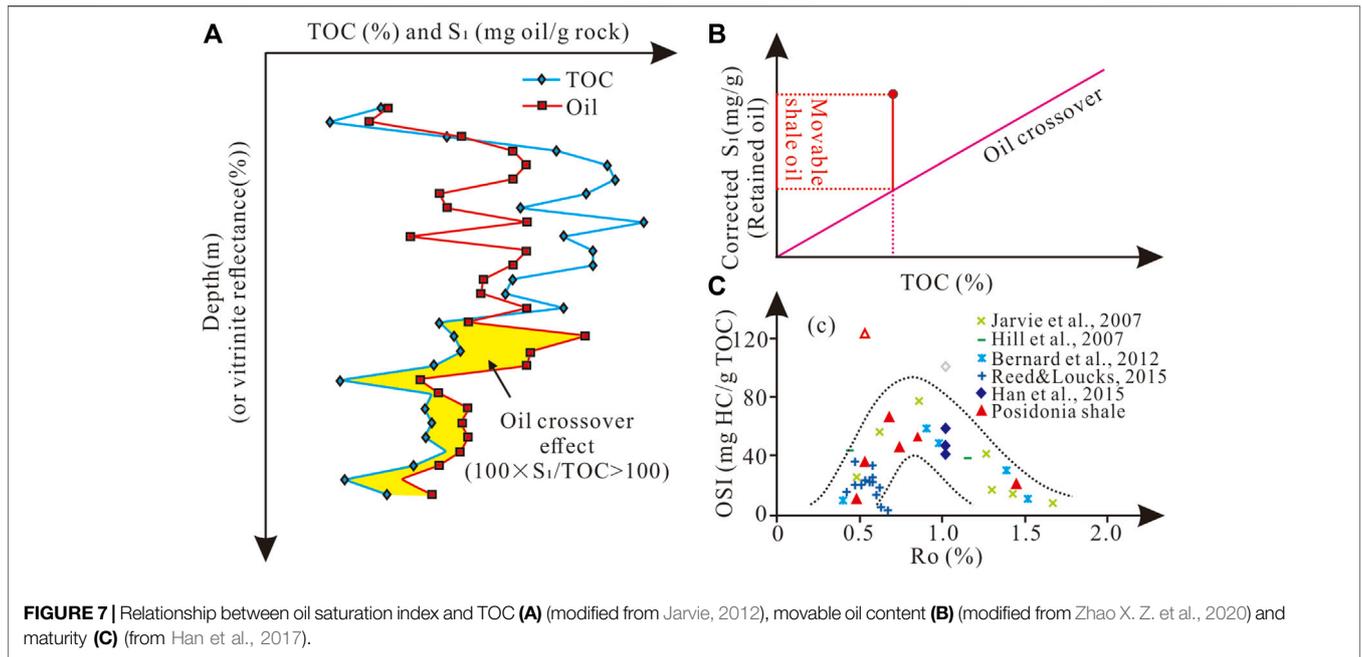
The light components contained in macropores and connected pore systems in the free state can be released at lower temperatures. In contrast, the heavy components in kerogen, and micropores and disconnected pore systems in the adsorption state can only be released at higher temperatures or when the temperature of organic matter cracking is reached (Jiang Q. G. et al., 2016). Therefore, the amount of movable shale oil can be evaluated by the thermally released hydrocarbon peak obtained under the constant-heating rate mode. Maende (2016) noted in the HAWK Petroleum Assessment Method that the movable oil content is the sum of Oil-1, Oil-2, Oil-3 and Oil-4 (**Figure 8A**). Jiang Q. G. et al. (2016) and Li J. B. et al. (2020a) considered that the thermally released hydrocarbon peak (S_{1-1}) at 200°C could represent the actual movable oil content, and the maximum movable oil content is the sum of S_{1-1} and S_{1-2} (at 350°C) (**Figure 8B**). Romero-Sarmiento (2019) proposed that sorbed liquid hydrocarbons is adsorbed on the residual solid OM, and thus the movable oil content of shales can be determined according to the area difference of thermal peaks (Sh0 (at 100–200°C) and Sh1 (at 200–350°C)) of whole rock sample and the corresponding isolated OM (**Figures 8C,D**). Chen Z. H. et al. (2019) and Li M. W. et al. (2020) applied the thermally released hydrocarbon peak (S_{1a}) at or below 300°C to represent the residual free hydrocarbons (**Figure 8E**) and believed that the shale oil discounted by the critical saturation is not limited by adsorption forces and nanopore bonds but exhibits fluidity (**Eq.** 7). Gentzis et al. (2021) thought that L1, L2 and a part of L3 represented movable oil, whereas the remaining L3 and L4 containing heavy n-alkanes, resins, asphaltenes and NSO compounds represented immovable oil (**Figure 8F**). Multistep pyrolysis method has low cost and easy operation, but it should be pointed out that the recovery of light hydrocarbon loss is necessary.

$$\varnothing_{mob} = \begin{cases} 0, & S_{1c} \leq \widetilde{TOC} \\ S_{1c} - \widetilde{TOC}, & S_1 > \widetilde{TOC} \end{cases} \qquad (7)$$

where S_{1c} is total free hydrocarbons after light hydrocarbon correction, $\widetilde{TOC}$ represents the amount of adsorption discount (mg HC/g TOC), which is equivalent to the percentage content of TOC in the sample.

NMR Method
A shale is characterized by complex porous media and multiple fluid occurrences (oil, gas, water and kerogen). The standard T_2 relaxation time distribution obtained by 1D NMR provides limited information, and signal overlap between the different fluids is severe (Birdwell and Washburn, 2015). Although T_2-D can be used to distinguish the fluid phase (oil, gas and water) in shales, the solid-like organic matter signal and kerogen signal in micro/nanopores cannot be effectively distinguished (Li J. B. et al., 2018; Bai et al., 2019; Song and Kausik, 2019). In contrast, 2D NMR, especially high-frequency 2D NMR, can improve the detection ability of trace signals and can more efficiently distinguish light oil, heavy components, kerogen, bound water and other fluids in shales. Specifically, kerogen (with high T_1) and structural water have shorter T_2 and wider

FIGURE 7 | Relationship between oil saturation index and TOC **(A)** (modified from Jarvie, 2012), movable oil content **(B)** (modified from Zhao X. Z. et al., 2020) and maturity **(C)** (from Han et al., 2017).

T_1, oil generally has a higher T_1/T_2 ratio than water (with low T_1), and the T_2 value of adsorbed oil is lower than that of movable oil (Li J. B. et al., 2018; Khatibi et al., 2019; Song and Kausik, 2019; Zhang P. F. et al., 2020) (**Figure 9A**). Based on the principle that 2D NMR can effectively distinguish hydrogen nuclei of fluids in different occurrence states, researchers have combined 2D NMR with geochemical experiments, such as rock pyrolysis, solvent extraction, and quantitative grain fluorescence on extract, to comprehensively analyze the content of movable shale oil (Bai et al., 2019; Liu B. et al., 2019; Li J. B. et al., 2020a; Gentzis et al., 2021). For example, Li J. B. et al. (2020a) extracted organic hydrogen T_2 spectra of kerogen, adsorbed oil and free oil at T_1 intervals corresponding to the original samples, samples pyrolyzed at 350°C and extracted samples. Their accumulative amplitude determined the T_2 cutoff values of free oil and adsorbed oil, and a nondestructive method for the direct evaluation of the free oil content was then provided (**Figures 9B,C**). However, it should be noted that the threshold value of the T_1-T_2 spectrum is related to the echo interval and frequency of the instrument itself (Nicot et al., 2016; Song and Kausik, 2019). The temperature and state of the samples and the magnetic minerals in shales would change the distribution of signal response interval (Bai et al., 2019). Furthermore, it is difficult to define the boundary of the T_1/T_2 ratio of movable and nonmovable fluids, which may lead to uncertainty in movable oil evaluation. Overall, for different testing method, they both have advantages and limitations, for accurate desripting movable oil content, various methods should be using synthetically.

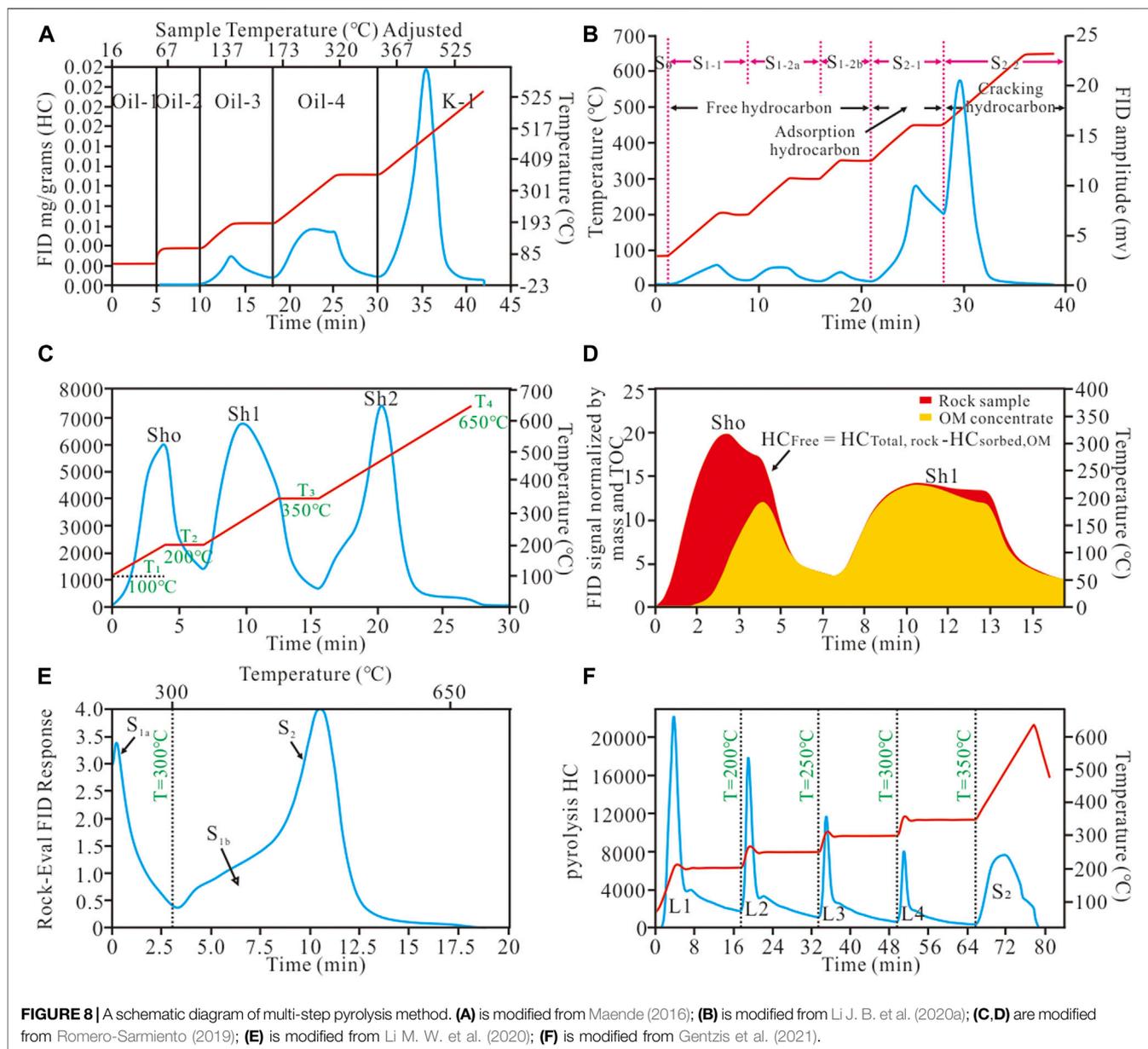## Adsorption-swelling Calculation Method

The shale oil adsorbed onto minerals and kerogen is usually immovable, and the movable oil content can be regarded as the difference between the total oil content and the adsorption-swelling oil content. Because the adsorption capacity of kerogen is much higher than that of minerals for shale oil, previous studies have mainly focused on the calculation of the adsorption and swelling capacities of kerogen (Wei et al., 2012; Tian et al., 2014), but this has caused an overestimation of the movable oil content. Therefore, Li et al. (2016) proposed the adsorption potential S_p model (**Eq. 8**) to calculate the oil adsorption amount in shale, and the difference between S_p and S_1 is suitable within a broader range of TOC and maturity levels (Zou et al., 2018). The adsorption-swelling oil quantity (Q_{a-s}) can also be calculated *via* molecular dynamics simulations (**Eq. 9**) (Tian et al., 2017; Tian et al., 2020). The swelling capacity of kerogen (Q_S) is calculated according to the shale oil density curve for kerogen. According to the density curve and specific surface area of shale oil in kerogen and mineral pores, the adsorbed oil quantity (Q_a) can be deduced. However, the adsorption-swelling calculation method is primarily a simplified model of shale under geological conditions. There may be differences between the premise and assumed parameters and the geological conditions, which results in insufficiently accurate calculations of adsorption-swelling oil content. Optimization of this model is a future research direction.

$$S_p = p_o x_o + \left[\frac{\varphi}{\varphi_0}\right]^{2/3} \sum_{i=1}^{n} p_i x_i \qquad (8)$$

$$Q_{a-s} = Q_s + Q_a = \int_{L_{o1}}^{L_{o2}} S_{ko}\rho_{ko} dL + \int_{L_{k2}}^{L_{k1}} S_{ko}\rho_{ko} dL + \int_{L_{m2}}^{L_{m1}} S_{mo}\rho_{mo} dL \quad (9)$$

where p_O and x_O are the proportion and adsorption capacity of OM respectively; p_i and x_i are the proportion of the ith mineral and its adsorbed oil amount respectively; $p_o + \sum_{i=1}^{n} p_i = 1$; φ and φ_o is porosity and shale initial porosity respectively; L_{o1} and L_{o2}

FIGURE 8 | A schematic diagram of multi-step pyrolysis method. **(A)** is modified from Maende (2016); **(B)** is modified from Li J. B. et al. (2020a); **(C,D)** are modified from Romero-Sarmiento (2019); **(E)** is modified from Li M. W. et al. (2020); **(F)** is modified from Gentzis et al. (2021).
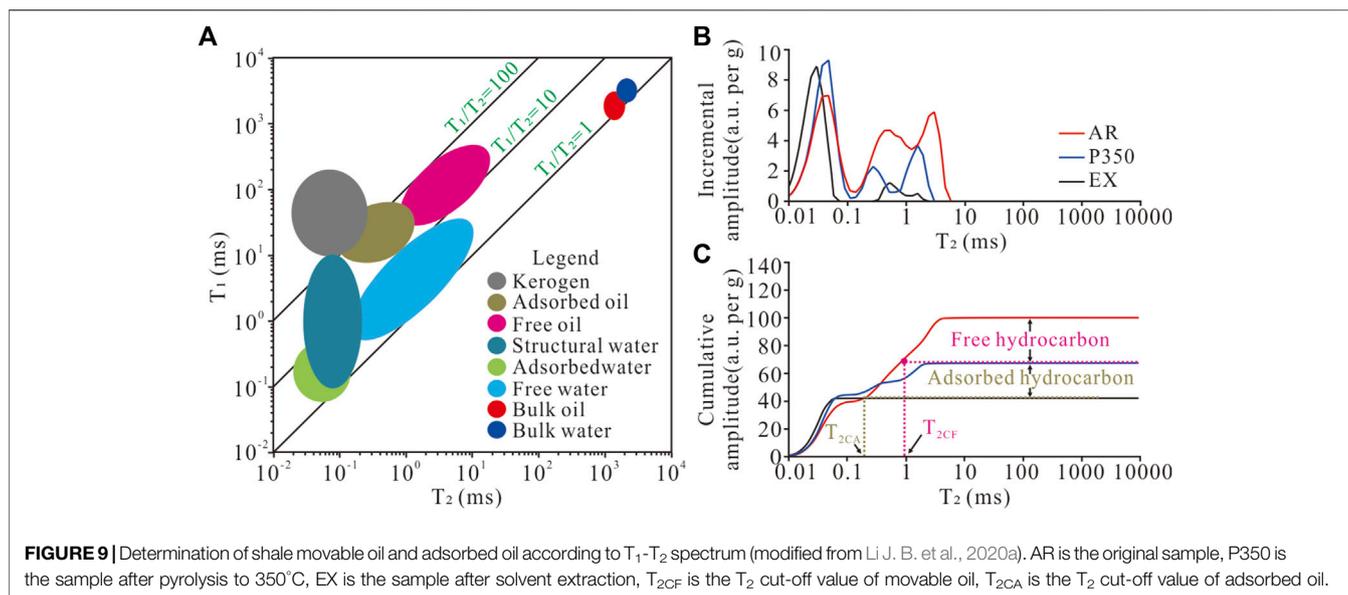
are the starting and ending positions of the intersection of kerogen density curve and shale oil density curve respectively; L_{k1} and L_{k2} are the starting point and end of kerogen adsorption layer respectively; L_{m1} and L_{m2} are the starting point and end of mineral component adsorption layer respectively; S_{ko} is the cross-sectional area of swelling and adsorption model of shale oil in kerogen, ρ_{ko} is the density curve of shale oil, S_{mo} is the adsorption model area of shale oil in mineral pores, and ρ_{mo} is the density curve of shale oil in mineral pores.

Influencing Factors of Movable Oil

Great effort has been made to explore the influencing factors of the shale oil mobility through various means of production and

experimental analysis methods. It is recognized that occurrences of retained oil in shales have a great influence on its fluidity. Adsorption-swelling oil occurs in the form of high-density solid-like or embedded kerogen on the surface of organic and inorganic pores (Wang et al., 2015b), and it is immovable without additional forces (Zhao X. Y. et al., 2021). The shale organic matter abundance exerts two impacts on the shale oil mobility. Even considering shale hydrocarbon expulsion, a high TOC is still beneficial to an increase in the shale oil and movable oil contents (Lu et al., 2012; Hu et al., 2021; Zhao W. Z. et al., 2021). However, in shales with the same oil content, an increase in the TOC content suggests a decrease in the movable oil content (Wang et al., 2019b). The relationship between the organic matter type and movable oil indicates that a higher oil generating capacity per

FIGURE 9 | Determination of shale movable oil and adsorbed oil according to T₁-T₂ spectrum (modified from Li J. B. et al., 2020a). AR is the original sample, P350 is the sample after pyrolysis to 350°C, EX is the sample after solvent extraction, T_{2CF} is the T₂ cut-off value of movable oil, T_{2CA} is the T₂ cut-off value of adsorbed oil.

unit of organic carbon means a higher movable oil content (He et al., 2019). It has been reported that the proportion of movable oil will increases with increasing burial depth. This phenomenon is related to the decrease in oil viscosity and density due to increasing temperature and light components (Wang et al., 2019b; Scheeder et al., 2020; Zhao W. Z. et al., 2021), which is conducive to a reduction in the oil film thickness and a relative increase in free oil in pores with the same pore size (Liu Y. S. et al., 2021). The increase in thermal maturity also leads to a decrease in the adsorption and swelling capacities of kerogen (Song et al., 2015; Wang et al., 2015b; Wang et al., 2019b). Li J. Q. et al. (2017) reported that the decrease in adsorption capacity could be attributed to the reduction in TOC content with increasing maturity. Wang et al. (2015b), based on molecular dynamics simulation analysis, proposed that with increasing maturity, the number of carbonyl in kerogen gradually decreases, which leads to the weakening of the adsorption capacity of kerogen for alkanes. Zhao X. Z. et al. (2020) conducted thermal simulation and kerogen swelling experiments on Paleogene shales obtained from the Huanghua depression of the Bohai Bay Basin and observed that an middle thermal maturity is the superior evolution stage for movable oil enrichment in lacustrine shale, which was attributed to the optimum matching of hydrocarbon generation and organic matter adsorption-swelling.

Mineral particles and composition play specific roles in controlling movable shale oil. Overall, although intergranular pores can be formed among clay minerals, tiny intergranular pores and the high surface adsorption capacity of clay minerals hinder the storage of movable liquid hydrocarbons (Su et al., 2018; Ning et al., 2020). The adsorption affinity of quartz and carbonate minerals for oil is low (Raji et al., 2015; Li et al., 2016), and the increase in their contents promotes the development of microcracks (Ougier-Simonin et al., 2016) and the preservation of macropores (Zhang P. L. et al., 2021), which facilitate the occurrence of mobile liquid hydrocarbons. However, Hu et al. (2021) analyzed the lacustrine shale of the Paleogene Shahejie

Formation in the Dongpu Sag of the Bohai Bay Basin. Their results revealed that the movable oil content first increases and then decreases with the content of clay minerals (25% as the inflection point) and quartz minerals (15% as the inflection point), which depends on the coupling effect of the mineral content on the porosity, adsorption capacity and TOC content. In addition, due to the petroleum fractionation effect, feldspar-quartz or carbonate laminae interbedded with organic-rich laminae at the microscale and interbedded shale, sandstone, carbonate, and mixed rock layers in shale strata at the macroscale contain more light oil components that easily flow (Jarvie, 2014; Li J. Q. et al., 2018; Fan and Shi, 2019; Pan et al., 2019; Liu B. et al., 2021).

Shale reservoir conditions are fundamental to the flow ability of shale oil. Bao (2018) speculated that shales within the oil generation window and a porosity higher than 6.5% promoted the storage of movable oil through the relationship between the OSI and porosity for the Paleogene shale in the Dongying Sag. The shale pore structure is a crucial factor controlling the shale oil mobility (Davudov et al., 2020; Jiang et al., 2020; Liu et al., 2020; Ning et al., 2020). Zou et al., 2015 found that oil cannot flow through pores below the lower limit of the flow threshold (20 nm) through simulations of a nanoporous template with a controllable pore diameter. Wang et al. (2015a), through adsorption simulations of alkanes onto a graphene surface (oil-wet), proposed that alkanes only flowed after exceeding the critical pore size. Conversely, they all occurred in the adsorption state. The pore size of shale reservoirs should exceed the flow threshold, which is a necessary condition for movable shale oil. The proportion of movable oil gradually increases with increasing pore size (Zhang P. F. et al., 2020) because the pore connectivity of macropores is higher and provides a considerable pore volume for movable oil (Li T. W. et al., 2017; Jiang et al., 2020; Ning et al., 2020), and the diffusion coefficient of oil increases with increasing pore diameter (Wang H. et al., 2016; Zhang et al., 2019). When the pore throat radius is large, the diffusion motion of

hydrocarbon molecules of different sizes in throats is not restricted by the diffusion energy barrier (Jiang et al., 2018). Cui and Cheng (2017) suggested that movable shale oil was also related to the porosity and pore size of organic pores, and the movable oil content decreased with increasing organic porosity ratio. The porosity and permeability of shales are low, and fractures can effectively improve the seepage capacity of shale reservoirs (Soeder and Borglum, 2019). Microfractures in shales are conducive to increasing the shale movable oil proportion and effective production (Song et al., 2020). Moreover, flow experiments have demonstrated that the shale oil fluidity is related to the fracture strength and direction, and bedding microfractures play an essential role in shale oil migration (Xie et al., 2019).

CONCLUSION

(1) The oil generated from organic-rich shales can be partly retained in themselves *via* through adsorption and swelling of kerogen, adsorption onto minerals and storage in pores. These mechanisms have been applied to explain to oil retention in shales under geological conditions, while the relative thermal dynamics is looked forward to further development.

(2) Quite a few methods have been developed to characterize and evaluate the oil in shales. The pyrolysis, thermal simulation experiment and material balance methods are most common use to quantify the oil content in shales.

(3) The shale oil retention capacity is bascially controlled by the organic matter abundance and properties (type and maturity), mineral composition, oil storage space, shale thickness and preservation conditions, but inconsistent

recoginitions exist, and are mainly from different scale research. It is necessary to strengthen a comprehensive study from the microscale to the macroscale.

(4) The study on the movable oil in shales still remains at the exploratory stage.

Although a few method are believed to be effective to estimate the movable oil content in shales, their limitations indicate needs for the supplement and verification of geological data. Especially, the influencing factors of shale movable oil are complex and variable. More accurate evaluation parameters and correction methods on this topic will become a research focus.

AUTHOR CONTRIBUTIONS

YF: Investigation, Writing - Original Draft. XX: Conceptualization, Methodology, Review and Editing. EW: Review and Editing. JS: Review and Editing. PG: Review. All authors contributed to the article and approved the submitted version.

FUNDING

ACKNOWLEDGMENTS

REFERENCES

Abrams, M. A., Gong, C., Garnier, C., and Sephton, M. A. (2017). A New Thermal Extraction Protocol to Evaluate Liquid Rich Unconventional Oil in Place and Iin-Ssitu Fluid Chemistry. *Mar. Pet. Geology.* 88, 659–675. doi:10.1016/j.marpetgeo.2017.09.014

Alfi, M., Yan, B., Cao, Y., An, C., Wang, Y., He, J., and Killough, J. E. (2014). "How to Improve Our Understanding of Gas and Oil Production Mechanisms in Liquid-Rich Shale," in SPE Annual Technical Conferences and Exhibition, Amsterdam, Netherlands, October 27–29, 2014. doi:10.2118/170959-MS

Bai, G. P., Qiu, H. H., Deng, Z. Z., Wang, W. Y., and Chen, J. (2020). Distribution and Main Controls for Shale Oil Resources in USA. *Pet. Geology. Exp.* 42 (04), 524–532. doi:10.11781/sysydz202004524 (in Chinese with English Abstract).

Bai, J., Xu, X. Y., and Chen, S. (2017). Analysis of Controlling Factors of Shale Oil Renrichment and Recoverable Capacity in continental Shale, A Case Study from Qingshankou Formation. *Geol. Rev.* 63 (S1), 117–118. doi:10.16509/j.georeview.2017.s1.056 (in Chinese with English Abstract).

Bai, L. H., Liu, B., Chi, Y. A., Jin, L., Yang, L., and Gao, S. (2019). Application of 2-D NMR Technique to Characterize Organic Matter in Shale deposit -A Case Study from the Qingshankou Formation in Southern Songliao Basin. *Oil Gas Geology.* 1–12. (in Chinese with English Abstract).

Bao, Y. S. (2018). Effective Reservoir Spaces of Paleogene Shale Oil in the Dongying Depression, Bohai Bay Basin. *Pet. Geology. Exp.* 40 (04), 479–484. doi:10.11781/sysydz201804479 (in Chinese with English Abstract).

Behar, F., Beaumont, V., and De B. Penteado, H. L. (2001). Rock-Eval 6 Technology: Performances and Developments. *Oil Gas Sci. Technol. - Rev. IFP* 56 (2), 111–134. doi:10.2516/ogst:2001013

Beti, D. R., Panja, P., Jiang, C., Milovic, M., Robinson, R., Ring, T. A., et al. (2020). Change in Hydrocarbon Composition in Rock Samples as a Function of Time: A Thermodynamic Evaporation Model. *J. Nat. Gas Sci. Eng.* 77, 103238. doi:10.1016/j.jngse.2020.103238

Birdwell, J. E., and Washburn, K. E. (2015). Multivariate Analysis Relating Oil Shale Geochemical Properties to NMR Relaxometry. *Energy Fuels* 29, 2234–2243. doi:10.1021/ef502828k

Burnham, A. K. (2017). *Global Chemical Kinetics of Fossil Fuels: How to Model Maturation and Pyrolysis.* Switzerland: Springer, 75–105. doi:10.1007/978-3-319-49634-4

Cao, H., Zou, Y.-R., Lei, Y., Xi, D., Wan, X., and Peng, P. A. (2017). Shale Oil Assessment for the Songliao Basin, Northeastern China, Using Oil Generation-Sorption Method. *Energy Fuels* 31 (5), 4826–4842. doi:10.1021/acs.energyfuels.7b00098

Cao, Z., Jiang, H., Zeng, J. H., Saibi, H., Lu, T. Z., Xie, X. M., et al. (2021). Nanoscale Liquid Hydrocarbon Adsorption on Clay Minerals: A Molecular Dynamics Simulation of Shale Oils. *Chem. Eng. J.* 420, 127578. doi:10.1016/j.cej.2020.127578

Cardott, B. J. (2012). Thermal Maturity of Woodford Shale Gas and Oil Plays, Oklahoma, USA. *Int. J. Coal Geology.* 103, 109–119. doi:10.1016/j.coal.2012.06.004

Carr, A. D. (1999). A Vitrinite Reflectance Kinetic Model Incorporating Overpressure Retardation. *Mar. Pet. Geology.* 16 (4), 355–377. doi:10.1016/S0264-8172(98)00075-0

Chen, G. H., Lu, S. F., Zhang, J. F., Pervukhina, M., Liu, K. Y., Wang, M., et al. (2018). A method for determining oil-bearing pore size distribution in shales: A case study from the Damintun Sag, China. *J. Pet. Sci. Eng.* 166, 673–678. doi:10.1016/j.petrol.2018.03.082

Chen, J. Q., Pang, X. Q., Pang, H., Chen, Z. H., and Jiang, C. Q. (2018). Hydrocarbon Evaporative Loss Evaluation of Lacustrine Shale Oil Based on Mass Balance Method: Permian Lucaogou Formation in Jimusaer Depression, Junggar Basin. *Mar. Pet. Geology.* 91, 422–431. doi:10.1016/j.marpetgeo.2018.01.021

Chen, J. P., Sun, Y. G., Zhong, N. N., Huang, Z. K., Deng, C. P., Xie, L. J., et al. (2014). The Efficiency and Model of Petroleum Expulsion from the Lacustrine Source Rocks Within Geological Frame. *Acta Geologica Sinica* 88 (11), 2005–2032. doi:10.1111/1755-6724.12373_3 (in Chinese with English Abstract).

Chen, L., Jiang, Z. X., Liu, Q. X., Jiang, S., Liu, K. Y., Tan, J. Q., et al. (2019a). Mechanism of Shale Gas Occurrence: Insights from Comparative Study on Pore Structures of Marine and Lacustrine Shales. *Mar. Pet. Geology.* 104, 200–216. doi:10.1016/j.marpetgeo.2019.03.027

Chen, L., Liu, K. Y., Jiang, S., Huang, H. X., Tan, J. Q., and Zuo, L. (2021). Effect of Adsorbed Phase Density on the Correction of Methane Excess Adsorption to Absolute Adsorption in Shale. *Chem. Eng. J.* 420, 127678. doi:10.1016/j.cej.2020.127678

Chen, L., Zuo, L., Jiang, Z. X., Jiang, S., Liu, K. Y., Tan, J. Q., et al. (2019b). Mechanisms of Shale Gas Adsorption: Evidence from Thermodynamics and Kinetics Study of Methane Adsorption on Shale. *Chem. Eng. J.* 361, 559–570. doi:10.1016/j.cej.2018.11.185

Chen, Y. Y., Lin, S. H., Bai, B., Zhang, T. S., Pang, Z. L., Tao, S. Z., et al. (2020). Effects of Petroleum Retention and Migration Within the Triassic Chang 7 Member of the Ordos Basin, China. *Int. J. Coal Geology.* 225, 103502. doi:10.1016/j.coal.2020.103502

Chen, Z. H., Li, M. W., and Jiang, C. Q. (2019). Shale Oil Resource Potential and Mobility Assessment: A Case Study of Upper Devonian Duvernay Shale in the Western Canada Sedimentary Basin. *Oil Gas Geology.* 40 (6), 459–468. doi:10.11743/ogg20190302 (in Chinese with English Abstract).

Chen, Z. H., Zha, M., and Jin, Q. (2004). An Investigation on Generation and Expulsion of Hydrocarbon from Source Rocks of the Shahejie Formation in the Well Niu-38, Dongying Depression. *Scientia Geologica Sinica* 39 (3), 356–366. (in Chinese with English Abstract).

Chen, Z. H., and Jiang, C. Q. (2015). A Data Driven Model for Studying Kerogen Kinetics with Application Examples from Canadian Sedimentary Basins. *Mar. Pet. Geol.* 67, 795–807. doi:10.1016/j.marpetgeo.2015.07.004

Chen, Z. H., and Jiang, C. Q. (2016). A Revised Method for Organic Porosity Estimation in Shale Reservoirs using Rock-Eval data: Example from Duvernay Formation in the Western Canada Sedimentary Basin. *AAPG Bull.* 100, 405–422. doi:10.1306/08261514173

Chen, Z. H., Liu, X. J., and Jiang, C. Q. (2017). Quick Evaluation of Source Rock Kerogen Kinetics Using Hydrocarbon Pyrograms from Regular Rock-Eval Analysis. *Energy Fuels* 31 (2), 1832–1841. doi:10.1021/acs.energyfuels.6b01569

Cooles, G. P., Mackenzie, A. S., and Quigley, T. M. (1986). Calculation of Petroleum Masses Generated and Expelled from Source Rocks. *Org. Geochem.* 10 (1-3), 235–245. doi:10.1016/0146-6380(86)90026-4

Cui, J., and Cheng, L. (2017). A Theoretical Study of the Occurrence State of Shale Oil Based on the Pore Sizes of Mixed Gaussian Distribution. *Fuel* 206, 564–571. doi:10.1016/j.fuel.2017.06.047

Davudov, D., Moghanloo, R. G., and Zhang, Y. (2020). Interplay Between Pore Connectivity and Permeability in Shale Sample. *Int. J. Coal Geology.* 220, 103427. doi:10.1016/j.coal.2020.103427

Du, J. Z., Cai, J. G., Lei, T. Z., and Li, Y. L. (2021). Diversified Roles of mineral Transformation in Controlling Hydrocarbon Generation Process, Mechanism, and Pattern. *Geosci. Front.* 12 (2), 725–736. doi:10.1016/j.gsf.2020.08.009

Du, J. H., Hu, S. Y., Pang, Z. L., Lin, S. H., and Zhu, R. K. (2019). The Types, Potentials and Prospects of Continental Shale Oil in China. *China Pet. Exploration* 24 (05), 560–568. doi:10.3969/j.issn.1672-7703.2019.05.003 (in Chinese with English Abstract).

Dudášová, D., Sébastien, S., Hemmingsen, P. V., and Sjöblom, J. (2008). Study of Asphaltenes Adsorption onto Different Minerals and Clays: Part 1. Experimental Adsorption with UV Depletion Detection. *Colloids Surf. A: Physicochemical Eng. Aspects* 317 (1-3), 1–9. doi:10.1016/j.colsurfa.2007.09.023

Ertas, D., Kelemen, S. R., and Halsey, T. C. (2006). Petroleum Expulsion Part 1. Theory of Kerogen Swelling in Multicomponent Solvents. *Energy Fuels* 20 (1), 295–300. doi:10.1021/ef058024k

Eseme, E., Krooss, B. M., and Littke, R. (2012). Evolution of Petrophysical Properties of Oil Shales During High-Temperature Compaction Tests: Implications for Petroleum Expulsion. *Mar. Pet. Geology.* 31 (1), 110–124. doi:10.1016/j.marpetgeo.2011.11.005

Fan, B., and Shi, L. (2019). Deep-Lacustrine Shale Heterogeneity and its Impact on Hydrocarbon Generation, Expulsion, and Retention: A Case Study from the Upper Triassic Yanchang Formation, Ordos Basin, China. *Nat. Resour. Res.* 28, 241–257. doi:10.1007/s11053-018-9387-2

Fu, X. F., Shi, H. D., Meng, Q. A., Liu, B., Liang, J. P., He, J. L., et al. (2020). Controlling Effects of the Structure and Deposition on the Shale Oil Enrichment: Taking Formation Qn1in the Central Depression of Songliao Basin as an Instance. *Pet. Geology. Oilfield Develop. Daqing* 39 (03), 56–71. doi:10.19597/J.ISSN.1000-3754.202005011 (in Chinese with English Abstract).

Fu, X. F., Wu, T., Lv, Y. F., Liu, S. B., Tian, H., and Lu, M. X. (2018). Research Status and Development Trend of the Reservoir Caprock Sealing Properties. *Oil Gas Geology.* 39 (03), 454–471. doi:10.11743/ogg20180304 (in Chinese with English Abstract).

Gao, Z. Y., Fan, Y. P., Hu, Q. H., Jiang, Z. X., Cheng, Y., and Xuan, Q. X. (2019). A Review of Shale Wettability Characterization Using Spontaneous Imbibition Experiments. *Mar. Pet. Geology.* 109, 330–338. doi:10.1016/j.marpetgeo.2019.06.035

Gentzis, T., Carvajal-Ortiz, H., Harry Xie, Z., Hackley, P. C., and Fowler, H. (2021). An Integrated Geochemical, Spectroscopic, and Petrographic Approach to Examining the Producibility of Hydrocarbons from Liquids-Rich Unconventional Formations. *Fuel* 298, 120357. doi:10.1016/j.fuel.2021.120357

Ghanizadeh, A., Clarkson, C. R., Clarke, K. M., Yang, Z., Rashidi, B., Vahedian, A., et al. (2020). Effects of Entrained Hydrocarbon and Organic-Matter Components on Reservoir Quality of Organic-Rich Shales: Implications for "Sweet Spot" Identification and Enhanced-Oil-Recovery Applications in the Duvernay Formation (Canada). *SPE J.* 25, 1351–1376. doi:10.2118/189787-pa

Hadad, Y. T., Hakimi, M. H., Abdullah, W. H., and Makeen, Y. M. (2017). Basin Modeling of the Late Miocene Zeit Source Rock in the Sudanese Portion of Red Sea Basin: Implication for Hydrocarbon Generation and Expulsion History. *Mar. Pet. Geology.* 84, 311–322. doi:10.1016/j.marpetgeo.2017.04.002

Han, W. Z., Zhao, W. Z., Jin, F. M., Pu, X. G., Chen, S. Y., Mou, L. G., et al. (2021). Sweet Spots Evaluation and Exploration of Lacustrine Shale Oil of the 2nd Member of Paleogene Kongdian Formation in Cangdong Sag, Dagang Oilfield, China. *Petrol. Explor. Dev.* 48 (4), 777–786. doi:10.11698/PED.2021.04.10

Han, Y. J., Horsfield, B., Wirth, R., Mahlstedt, N., and Bernard, S. (2017). Oil Retention and Porosity Evolution in Organic-Rich Shales. *AAPG Bull.* 101 (6), 807–827. doi:10.1306/09221616069

Han, Y. J., Mahlstedt, N., and Horsfield, B. (2015). The Barnett Shale: Compositional Fractionation Associated with Intraformational Petroleum Migration, Retention, and Expulsion. *AAPG Bull.* 99 (12), 2173–2202. doi:10.1306/06231514113

He, T. H., Li, W. H., Tan, Z. Z., Wang, Y., Zhang, W. B., and Zhang, X. W. (2019). Mechanism of Shale Oil Accumulation in the Hetaoyuan Formation from the Biyang Depression, Nanxiang Basin. *Oil Gas Geology.* 40 (6), 1259–1269. doi:10.11743/ogg20190610 (in Chinese with English Abstract).

Hou, L. H., Luo, X., Lin, S. H., Zhao, Z. Y., and Li, Y. (2021a). Quantitative Measurement of Retained Oil in Organic-Rich Shale-A Case Study on the Chang 7 Member in the Ordos Basin, China. *Front. Earth Sci.* 9, 662586. doi:10.3389/feart.2021.662586

Hou, L. H., Ma, W. Z., Luo, X., and Liu, J. Z. (2020). Characteristics and Quantitative Models for Hydrocarbon Generation-Retention-Production of Shale Under ICP Conditions: Example from the Chang 7 Member in the Ordos Basin. *Fuel* 279, 118497. doi:10.1016/j.fuel.2020.118497

Hou, L. H., Ma, W. J., Luo, X., Liu, J. Z., Liu, S. H., and Zhao, Z. Y. (2021b). Hydrocarbon Generation-Retention-Expulsion Mechanism and Shale Oil Producibility of the Permian Lucaogou Shale in the Junggar Basin as Simulated by Semi-open Pyrolysis Experiments. *Mar. Pet. Geology.* 125, 104880. doi:10.1016/j.marpetgeo.2020.104880

Hou, Q. J., Jin, Q., Li, P. P., Jiang, W. M., Zhang, F. J., and Tian, F. (2017). A Computational Method for Determining Oil Expulsion Efficiency Based on the

Ideal Effective Oil Expulsion Mode. *J. Petrol. Explor Prod. Technol.* 7, 925–931. doi:10.1007/s13202-017-0337-z

Hu, S. Y., Zhao, W. Z., Hou, L. H., Yang, Z., Zhu, R. K., Wu, S. T., et al. (2020). Development Potential and Technical Strategy of continental Shale Oil in China. *Pet. Exploration Develop.* 47 (4), 877–887. doi:10.1016/S1876-3804(20)60103-3

Hu, T., Pang, X. Q., Jiang, F. J., Wang, Q. F., Liu, X. H., Wang, Z., et al. (2021). Movable Oil Content Evaluation of Lacustrine Organic-Rich Shales: Methods and a Novel Quantitative Evaluation Model. *Earth-Science Rev.* 214, 103545. doi:10.1016/j.earscirev.2021.103545

Hu, T., Pang, X. Q., Jiang, S., Wang, Q. F., Zheng, X. W., Ding, X. G., et al. (2018). Oil Content Evaluation of Lacustrine Organic-Rich Shale with strong Heterogeneity: A Case Study of the Middle Permian Lucaogou Formation in Jimusaer Sag, Junggar Basin, NW China. *Fuel* 221, 196–205. doi:10.1016/j.fuel.2018.02.082

Hu, W. X., Yao, S. P., Lu, X. C., Wu, H. G., Sun, F. N., and Jin, J. (2019). Effects of Organic Matter Evolution on Oil Reservoir Property During Diagenesis of Typical Continental Shale Sequences. *Oil Gas Geology.* 40 (05), 947–956. doi:10.11743/ogg20190501 (in Chinese with English Abstract).

Huang, D. F. (1996). Advances in Hydrocarbon Generation Theory –(I) Immature Oils and Generating Hydrocarbon and Evolutionary Model. *Adv. Earth Sci.* (4), 2–10. (in Chinese with English Abstract).

Huang, W. B., Salad Hersi, O., Lu, S. F., and Deng, S. W. (2017). Quantitative Modelling of Hydrocarbon Expulsion and Quality Grading of Tight Oil Lacustrine Source Rocks: Case Study of Qingshankou 1 Member, central Depression, Southern Songliao Basin, China. *Mar. Pet. Geology.* 84, 34–48. doi:10.1016/j.marpetgeo.2017.03.021

Huang, Z. K., Hao, Y. Q., Li, S. J., Wo, Y. J., Sun, D. S., Li, M. W., et al. (2020). Oil-bearing Potential, Mobility Evaluation and Significance of Shale Oil in Chang 7 Shale System in the Ordos Basin: A Case Study of Well H317. *Geology. China* 47 (01), 210–219. doi:10.12029/gc20200117 (in Chinese with English Abstract).

Jarvie, D. M. (2014). Components and Processes Affecting Producibility and Commerciality of Shale Resource Systems. *Geologica Acta* 12 (4), 307–325. doi:10.1344/GeologicaActa2014.12.4.3

Jarvie, D. M. (2012). "Shale Resource Systems for Oil and GasPart 2 Shale-Oil Resource Systems," in *Shale Reservoirs-Giant Resources for the 21st century.* Editor J. A. Breyer (Tulsa: American Association of Petroleum Geologists), 97, 89–119. doi:10.1306/13321447M973489

Jiang, C. Q., Chen, Z. H., Mort, A., Milovic, M., Robinson, R., Stewart, R., et al. (2016). Hydrocarbon Evaporative Loss from Shale Core Samples as Revealed by Rock-Eval and Thermal Desorption-Gas Chromatography Analysis: Its Geochemical and Geological Implications. *Mar. Pet. Geology.* 70, 294–303. doi:10.1016/j.marpetgeo.2015.11.021

Jiang, N. H., Jia, F. Y., and Shen, J. M. (1986). The Primary Oil Migration and Effective Hydrocarbon Expelling Thickness of Source Rocks in Biyang Depression. *Pet. Explor. Dev.* (2), 19–24. (in Chinese with English Abstract).

Jiang, Q. G., Li, M. W., Ma, Y. Y., Cao, T. T., Liu, P., Qian, M. H., et al. (2018). Molecular Geochemical Evaluation of Shale Oil Mobility: A Case Study of Shale Oil in Jiyang Depression. *Pet. Geology. Exp.* 40 (06), 849–854. doi:10.11781/sysydz201806849 (in Chinese with English Abstract).

Jiang, Q. G., Li, M. W., Qian, M. H., Li, Z. M., Li, Z., Huang, Z. K., et al. (2016). Quantitative Characterization of Shale Oil in Different Occurrence States and its Application. *Pet. Geology. Exp.* 38 (06), 842–849. doi:10.11781/sysydz201606842 (in Chinese with English Abstract).

Jiang, Z. X., Li, T. W., Gong, H. J., Jiang, T., Chang, J. Q., Ning, C. X., et al. (2020). Characteristics of Low-Mature Shale Reservoirs in Zhanhua Sag and Their Influence on the Mobility of Shale Oil. *Acta Petrolei Sinica* 41 (12), 1587–1600. doi:10.7623/syxb202012011 (in Chinese with English Abstract).

Jin, J., Yang, Z., Chen, X. K., Li, L. L., Yang, H. X., Ju, Y. W., et al. (2021). Characteristics of Micro/nano Pores and Hydrocarbon Accumulation in a continental Shale Oil Reservoir-A Case Study of the Lucaogou Formation in the Jimsar Sag, Junggar Basin, Northwest China. *j nanosci nanotechnol* 21 (1), 262–273. doi:10.1166/jnn.2021.18749

Kelemen, S. R., Walters, C. C., Ertas, D., Freund, H., and Curry, D. J. (2006). Petroleum Expulsion Part 3. A Model of Chemically Driven Fractionation during Expulsion of Petroleum from Kerogen. *Energy Fuels* 20 (1), 309–319. doi:10.1021/ef058023s

Khatibi, S., Ostadhassan, M., Xie, Z. H., Gentzis, T., Bubach, B., Gan, Z., et al. (2019). NMR Relaxometry A New Approach to Detect Geochemical Properties of Organic Matter in Tight Shales. *Fuel* 235, 167–177. doi:10.1016/j.fuel.2018.07.100

Kumar, S., Ojha, K., Bastia, R., Garg, K., Das, S., and Mohanty, D. (2017). Evaluation of Eocene Source Rock for Potential Shale Oil and Gas Generation in north Cambay Basin, India. *Mar. Pet. Geology.* 88, 141–154. doi:10.1016/j.marpetgeo.2017.08.015

Larsen, J. W., and Li, S. (1997). An Initial Comparison of the Interactions of Type I and III Kerogens with Organic Liquids. *Org. Geochem.* 26 (5–6), 305–309. doi:10.1016/S0146-6380(97)00016-8

Larsen, J. W., and Li, S. (1994). Solvent Swelling Studies of Green River Kerogen. *Energy Fuels* 8 (4), 932–936. doi:10.1021/ef00046a017

Larsen, J. W., Parikh, H., and Michels, R. (2002). Changes in the Cross-Link Density of Paris Basin Toarcian Kerogen During Maturation. *Org. Geochem.* 33 (10), 1143–1152. doi:10.1016/S0146-6380(02)00102-X

Lewan, M. D., and Roy, S. (2011). Role of Water in Hydrocarbon Generation from Type-I Kerogen in Mahogany Oil Shale of the Green River Formation. *Org. Geochem.* 42 (1), 31–41. doi:10.1016/j.orggeochem.2010.10.004

Leythaeuser, D., Mackenzie, A., Schaefer, R. G., and BjorØy, M. (1984). A Novel Approach for Recognition and Quantification of Hydrocarbon Migration Effects in Shale-sandstone Sequences. *AAPG Bull.* 68 (2), 196–219. doi:10.1306/AD4609FE-16F7-11D7-8645000102C1865D

Li, C. R., Pang, X. Q., Huo, Z. P., Wang, E. Z., and Xue, N. (2020). A Revised Method for Reconstructing the Hydrocarbon Generation and Expulsion History and Evaluating the Hydrocarbon Resource Potential: Example from the First Member of the Qingshankou Formation in the Northern Songliao Basin, Northeast China. *Mar. Pet. Geology.* 121, 104577. doi:10.1016/j.marpetgeo.2020.104577

Li, H., Lu, J. L., Wang, B. H., Lu, K., Zhou, Y., Wang, M., et al. (2020). Critical Controlling Factors of Enrichment and High-Yield of Land Shale Oil. *Geoscience* 34 (04), 837–848. doi:10.19657/j.geoscience.1000-8527.2020.04.19 (in Chinese with English Abstract).

Li, J. B., Huang, W. B., Lu, S. F., Wang, M., Chen, G. H., Tian, W. C., et al. (2018). Nuclear Magnetic Resonance T1-T2 Map Division Method for Hydrogen-Bearing Components in Continental Shale. *Energy Fuels* 32 (9), 9043–9054. doi:10.1021/acs.energyfuels.8b01541

Li, J. B., Jiang, C. Q., Wang, M., Lu, S. F., Chen, Z. H., Chen, G. H., et al. (2020a). Adsorbed and Free Hydrocarbons in Unconventional Shale Reservoir: A New Insight from NMR T1-T2 Maps. *Mar. Pet. Geology.* 116, 104311. doi:10.1016/j.marpetgeo.2020.104311

Li, J. J., Wang, W. M., Cao, Q., Shi, Y. L., Yan, X. T., and Tian, S. S. (2015). Impact of Hydrocarbon Expulsion Efficiency of Continental Shale Upon Shale Oil Accumulations in Eastern China. *Mar. Pet. Geol.* 59, 467–479. doi:10.1016/j.marpetgeo.2014.10.002

Li, J. J., Liu, Z., Li, J. Q., Lu, S. F., Zhang, T. Q., Zhang, X. W., et al. (2018). Fractal Characteristics of Continental Shale Pores and its Significance to the Occurrence of Shale Oil in China: A Case Study of Biyang Depression. *Fractals* 26 (2), 1840008. doi:10.1142/S0218348X1840008X

Li, J. Q., Lu, S. F., Cai, J. C., Zhang, P. F., Xue, H. T., and Zhao, X. B. (2018). Adsorbed and Free Oil in Lacustrine Nanoporous Shale: A Theoretical Model and A Case Study. *Energy Fuels* 32 (12), 12247–12258. doi:10.1021/acs.energyfuels.8b02953

Li, J. Q., Lu, S. F., Xie, L. J., Zhang, J., Xue, H. T., Zhang, P. F., et al. (2017). Modeling of Hydrocarbon Adsorption on continental Oil Shale: A Case Study on N-Alkane. *Fuel* 206, 603–613. doi:10.1016/j.fuel.2017.06.017

Li, J., Ma, W., Wang, Y. F., Wang, D. L., Xie, Z. Y., Li, Z. S., et al. (2018). Modeling of the Whole Hydrocarbon-Generating Process of Sapropelic Source Rock. *Pet. Exploration Develop.* 45 (03), 461–471. doi:10.1016/S1876-3804(18)30051-X

Li, J. B., Wang, M., Chen, Z. H., Lu, S. F., Jiang, C. Q., Chen, G. H., et al. (2019). Evaluating the Total Oil Yield Using a Single Routine Rock-Eval experiment on As-Received Shales. *J. Anal. Appl. Pyrolysis* 144, 104707. doi:10.1016/j.jaap.2019.104707

Li, J. B., Wang, M., Lu, S. F., Chen, G. H., Tian, W. C., Jiang, C. Q., et al. (2020b). A New Method for Predicting Sweet Spots of Shale Oil Using Conventional Well Logs. *Mar. Pet. Geology.* 113, 104097. doi:10.1016/j.marpetgeo.2019.104097

Li, J., Wang, Y. F., Ma, W., Wang, D. L., Ma, C. H., and Li, Z. S. (2015). Evaluation on Occluded Hydrocarbon in Deep-Ultra Deep Ancient Source Rocks and its

Cracked Gas Resources. *Nat. Gas Industry B* 2 (6), 499–505. doi:10.1016/j.ngib.2015.12.003

Li, M. W., Chen, Z. H., Ma, X. X., Cao, T. T., Li, Z. M., and Jiang, Q. G. (2018). A Numerical Method for Calculating Total Oil Yield Using a Single Routine Rock-Eval Program: A Case Study of the Eocene Shahejie Formation in Dongying Depression, Bohai Bay Basin, China. *Int. J. Coal Geology.* 191, 49–65. doi:10.1016/j.coal.2018.03.004

Li, M. W., Chen, Z. H., Ma, X. X., Cao, T. T., Qian, M. H., Jiang, Q. G., et al. (2019a). Shale Oil Resource Potential and Oil Mobility Characteristics of the Eocene-Oligocene Shahejie Formation, Jiyang Super-depression, Bohai Bay Basin of China. *Int. J. Coal Geology.* 204, 130–143. doi:10.1016/j.coal.2019.01.013

Li, M. W., Chen, Z. H., Qian, M. H., Ma, X. X., Jiang, Q. G., Li, Z. M., et al. (2020). What Are in Pyrolysis S1 Peak and what Are Missed? Petroleum Compositional Characteristics Revealed from Programed Pyrolysis and Implications for Shale Oil Mobility and Resource Potential. *Int. J. Coal Geology.* 217, 103321. doi:10.1016/j.coal.2019.103321

Li, M. W., Ma, X. X., Jiang, Q. G., Li, Z. M., Pang, X. Q., and Zhang, C. T. (2019b). Enlightenment from Formation Conditions and Enrichment Characteristics of Marine Shale Oil in North America. *Pet. Geology. Recovery Efficiency* 26 (1), 13–28. doi:10.13673/j.cnki.cn37-1359/te.2019.01.002 (in Chinese with English Abstract).

Li, T. W., Jiang, Z. X., Xu, C. L., Liu, B., Liu, G. H., Wang, P. F., et al. (2017). Effect of Pore Structure on Shale Oil Accumulation in the Lower Third Member of the Shahejie Formation, Zhanhua Sag, Eastern China: Evidence from Gas Adsorption and Nuclear Magnetic Resonance. *Mar. Pet. Geology.* 88, 932–949. doi:10.1016/j.marpetgeo.2017.09.030

Li, X. N., Ren, J. H., Xin, M., Liang, H., Zhang, P., Ma, Q., et al. (2017). Discussions on Movable Hydrocarbons in Source-Rock Oil in the Second Member of Permian Lucaogou Formation, Santanghu Basin. *Xinjiang Pet. Geology.* 38 (03), 296–301. doi:10.7657/XJPG20170307 (in Chinese with English Abstract).

Li, Z. (2020). Comparison of oil-bearing properties and oil mobility of shale with different lithologies in continental basins: a case study of the upper fourth member of Paleogene Shahejie Formation in Dongying Sag, Bohai Bay Basin. *Petrol. Geol. Exp.* 42, 545–595. doi:10.11781/sysydz202004545 (in Chinese with English Abstract)

Li, Z., Zou, Y.-R., Xu, X.-Y., Sun, J.-N., Li, M., and Peng, P. A. (2016). Adsorption of Mudstone Source Rock for Shale Oil - Experiments, Model and a Case Study. *Org. Geochem.* 92, 55–62. doi:10.1016/j.orggeochem.2015.12.009

Liang, C., Cao, Y., Jiang, Z. X., Wu, J., Song, G. Q., and Wang, Y. S. (2017). Shale Oil Potential of Lacustrine Black Shale in the Eocene Dongying Depression: Implications for Geochemistry and Reservoir Characteristics. *AAPG Bull.* 101 (11), 1835–1858. doi:10.1306/01251715249

Liang, X. P., Jin, Z. J., Shpilman, A., Yin, J. Y., Liu, Q. Y., and Uspensky, B. (2019). Geological Characteristics and Latest Progress in Exploration and Development of Russian Shale Oil. *Oil Gas Geology.* 40 (03), 478–490. doi:10.11743/ogg20190304 (in Chinese with English Abstract).

Lin, H. X., Song, M. S., Wang, S. Z., and Zhang, K. H. (2020). Shale Oil Resource Evaluation in Complex Structural Belt of Superimposed Basin: A Case Study of Middle Permian Lucaogou Formation in Bogda Area,southeast Margin of Junggar Basin. *Pet. Geology. Recovery Efficiency* 27 (02), 7–17. doi:10.13673/j.cnki.cn37-1359/te.2020.02.002 (in Chinese with English Abstract).

Liu, B., Bai, L. H., Chi, Y. A., Jia, R., Fu, X. F., and Yang, L. (2019). Geochemical Characterization and Quantitative Evaluation of Shale Oil Reservoir by Two-Dimensional Nuclear Magnetic Resonance and Quantitative Grain Fluorescence on Extract: A Case Study from the Qingshankou Formation in Southern Songliao Basin, Northeast China. *Mar. Pet. Geology.* 109, 561–573. doi:10.1016/j.marpetgeo.2019.06.046

Liu, B., Shi, J. X., Fu, X. F., Lv, Y. F., Sun, X. D, Gong, L., et al. (2018). Petrological Characteristics and Shale Oil Enrichment of Lacustrine fine-grained Sedimentary System: A Case Study of Organic-Rich Shale in First Member of Cretaceous Qingshankou Formation in Gulong Sag, Songliao Basin, NE China. *Pet. Exploration Develop.* 45 (05), 884–894. doi:10.1016/s1876-3804(18)30091-0

Liu, B., Sun, J. H., Zhang, Y. Q., He, J. L., Fu, X. F., Yang, L., et al. (2021). Reservoir Space and Enrichment Model of Shale Oilin the First Member of Cretaceous Qingshankou Formationin the Changling Sag, Southern Songliao Basin, NE China. *Pet. Explor. Dev.* 48 (03), 521–535. doi:10.1016/s1876-3804(21)60049-6

Liu, C., Lu, S. F., and Xue, H. T. (2014). Variable-coefficient ΔlogR Model and its Application in Shale Organic Evaluation. *Prog. Geophys.* 29 (01), 312–317. doi:10.6038/pg20140144

Liu, H. M., Zhang, S., Bao, S. Y., Fang, Z. W., Yao, S. P., and Wang, Y. (2019). Geological Characteristics and Effectiveness of the Shale Oil Reservoir in Dongying Sag. *Oil Gas Geology.* 40 (3), 512–523. doi:10.11743/ogg20190307 (in Chinese with English Abstract).

Liu, X. P., Lai, J., Fan, X. C., Shu, H. L., Wang, G. C., Ma, X. Q., et al. (2020). Insights in the Pore Structure, Fluid Mobility and Oiliness in Oil Shales of Paleogene Funing Formation in Subei Basin, China. *Mar. Pet. Geol.* 114, 104228. doi:10.1016/j.marpetgeo.2020.104228

Liu, X. P., Zhan, J.-H., Lai, D. G., Liu, X. X., Zhang, Z. J., and Xu, G. W. (2015). Initial Pyrolysis Mechanism of Oil Shale Kerogen with Reactive Molecular Dynamics Simulation. *Energy Fuels* 29 (5), 2987–2997. doi:10.1021/acs.energyfuels.5b00084

Liu, X. Y., and Zhang, D. X. (2019). A Review of Phase Behavior Simulation of Hydrocarbons in Confined Space: Implications for Shale Oil and Shale Gas. *J. Nat. Gas Sci. Eng.* 68, 102901. doi:10.1016/j.jngse.2019.102901

Liu, Y. S., Dong, X. H., Chen, Z. X., Hou, Y. N., Luo, Q. L., and Chen, Y. H. (2021). A Novel Experimental Investigation on the Occurrence State of Fluids in Microscale Pores of Tight Reservoirs. *J. Pet. Sci. Eng.* 196, 107656. doi:10.1016/j.petrol.2020.107656

Lu, S. F., Huang, W. B., Chen, F. W., Li, J. J., Wang, M., Xue, H. T., et al. (2012). Classification and Evaluation Criteria of Shale Oil and Gas Resources: Discussion and Application. *Pet. Exploration Develop.* 39 (2), 268–276. doi:10.1016/S1876-3804(12)60042-1

Ma, W., Li, J., Wang, D. L., Wang, Y. F., Ma, C. H., Wang, Z. H., et al. (2016). Hydrocarbon Expulsion Efficiency of Source Rocks and its Influencing Factors. *Nat. Gas Geosci.* 27 (09), 1742–1751. doi:10.11764/j.issn.1672-1926.2016.09.1742 (in Chinese with English Abstract).

Ma, X. X., Zheng, L. J., Yu, X. L., Zhao, Z. X., and Li, Z. M. (2018). Effective Oil Expulsion Threshold of Argillaceous Source Rocks and Geological Significance of Shale Oil. *J. China Univ. Pet. (Edition Nat. Science)* 42 (1), 32–39. doi:10.3969/j.issn.1673-5005.2018.01.004 (in Chinese with English Abstract).

Maende, A. (2016). Wildcat Compositional Analysis for Conventional and Unconventional Reservoir Assessments, HAWK Petroleum Assessment Method (HAWK-PAM). Appl. Note 052016-1, 11p, Texas, Wildcat Technologies. Available at: https://www.wildcattechnologies.com/hawk-pam-petroleum-assessment.

Milliken, K. L., Zhang, T. W., Chen, J. P., and Ni, Y. Y. (2021). Mineral Diagenetic Control of Expulsion Efficiency in Organic-Rich Mudrocks, Bakken Formation (Devonian-Mississippian), Williston Basin, North Dakota, U.S.A. *Mar. Pet. Geology.* 127, 104869. doi:10.1016/j.marpetgeo.2020.104869

Mohammadi, M., and Sedighi, M. (2013). Modification of Langmuir Isotherm for the Adsorption of Asphaltene or Resin onto Calcite Mineral Surface: Comparison of Linear and Non-linear Methods. *Prot. Met. Phys. Chem. Surf.* 49 (4), 460–470. doi:10.1134/S2070205113040205

Nicot, B., Vorapalawut, N., Rousseau, B., Madariaga, L. F., Hamon, G., and Korb, J. P. (2016). Estimating Saturations in Organic Shales Using 2D NMR. *Petrophysics* 57 (1), 19–29.

Nie, H. K., Zhang, P. X., Bian, D. K., Wu, X. L., and Zhai, C. B. (2016). Oil Accumulation Characteristics of China continental Shale. *Earth Sci. Front.* 23 (02), 55–62. doi:10.13745/j.esf.2016.02.007 (in Chinese with English Abstract).

Nielsen, S. B., Clausen, O. R., and McGregor, E. (2017). basin%Ro: A Vitrinite Reflectance Model Derived from Basin and Laboratory Data. *Basin Res.* 29, 515–536. doi:10.1111/bre.12160

Ning, C. X., Ma, Z. L., Jiang, Z. X., Su, S. Y., Li, T. W., Zheng, L. J., et al. (2020). Effect of Shale Reservoir Characteristics on Shale Oil Movability in the Lower Third Member of the Shahejie Formation, Zhanhua Sag. *Acta Geologica Sinica - English Edition* 94 (02), 352–363. doi:10.1111/1755-6724.14284

Ougier-Simonin, A., Renard, F., Boehm, C., and Vidal-Gilbert, S. (2016). Microfracturing and Microporosity in Shales. *Earth-Science Rev.* 162, 198–226. doi:10.1016/j.earscirev.2016.09.006

Pan, S. Q., Zou, C. N., Li, J., Yang, Z., Liu, E., and Han, Y. (2019). Unconventional Shale Systems: A Comparative Study of the "In-Source Sweet Spot" Developed in the Lacustrine Chang 7 Shale and the marine Barnett Shale. *Mar. Pet. Geology.* 100, 540–550. doi:10.1016/j.marpetgeo.2018.12.015

Panahi, H., Kobchenko, M., Meakin, P., Dysthe, D. K., and Renard, F. (2019). Fluid Expulsion and Microfracturing During the Pyrolysis of an Organic Rich Shale. *Fuel* 235, 1–16. doi:10.1016/j.fuel.2018.07.069

Pang, X. Q., Li, M. W., Li, S. M., and Jin, Z. J. (2005). Geochemistry of Petroleum Systems in the Niuzhuang South Slope of Bohai Bay Basin: Part 3. Estimating Hydrocarbon Expulsion from the Shahejie Formation. *Org. Geochem.* 36, 497–510. doi:10.1016/j.orggeochem.2004.12.001

Pathak, M., Kweon, H., Deo, M., and Huang, H. (2017). Kerogen Swelling and Confinement: Its Implication on Fluid Thermodynamic Properties in Shales. *Sci. Rep.* 7, 12530. doi:10.1038/s41598-017-12982-4

Peng, W. L., Hu, G. Y., Liu, Q. Y., Jia, N., Fang, C. C., Gong, D. Y., et al. (2018). Research Status on Thermal Simulation Experiment and Several Issues of Concern. *J. Nat. Gas Geosci.* 3 (5), 283–293. doi:10.1016/j.jnggs.2018.11.006

Pepper, A. S. (1991). Estimating the Petroleum Expulsion Behaviour of Source Rocks: A Novel Quantitative Approach. *Geol. Soc. Lond. Spec. Publications* 59, 9–31. doi:10.1144/GSL.SP.1991.059.01.02

Peters, K. E., Burnham, A. K., Walters, C. C., and Schenk, O. (2018). Guidelines for Kinetic Input to Petroleum System Models from Open-System Pyrolysis. *Mar. Pet. Geology.* 92, 979–986. doi:10.1016/j.marpetgeo.2017.11.024

Piedrahita, J., and Aguilera, R. (2017). "Estimating Oil Saturation Index OSI from NMR Logging and Comparison with Rock-Eval Pyrolysis Measurements in a Shale Oil Reservoir," in The SPE Unconventional Resources Conference, Calgary, AB, Canada, February 15–16, 2017. doi:10.2118/185073-MS

Qian, K.-R., He, Z.-L., Liu, X.-W., and Chen, Y.-Q. (2018). Intelligent Prediction and Integral Analysis of Shale Oil and Gas Sweet Spots. *Pet. Sci.* 15, 744–755. doi:10.1007/s12182-018-0261-y

Qian, M. H., Jiang, Q. G., Li, M. W., Li, Z. M., Liu, P., Ma, Y. Y., et al. (2017). Quantitative Characterization of Extractable Organic Matter in Lacustrine Shale with Different Occurrences. *Pet. Geology. Exp.* 39 (02), 278–286. doi:10.11781/sysydz201702278 (in Chinese with English Abstract).

Qian, M. H., Jiang, Q. G., Li, M. W., Li, Z. M., and Liu, P. (2020). Three-dimensional Quantitative Fluorescence Analysis and Application in Shale. *Pet. Geology. Exp.* 42 (02), 311–318. doi:10.11781/sysydz202002311 (in Chinese with English Abstract).

Qiu, Z., Lu, B., Qiu, Z. S., Dong, D. Z., Wang, H. Y., Zhou, J., et al. (2016). Residual Accumulation and Resource Assessment of Shale Oil from the Permian Lucaogou Formation in Jimusar Sag. *Nat. Gas Geosci.* 27 (10), 1817–1827. doi:10.11764/j.issn.1672-1926.2016.10.1817 (in Chinese with English Abstract).

Raji, M., Gröcke, D. R., Greenwell, H. C., Gluyas, J. G., and Cornford, C. (2015). The Effect of Interbedding on Shale Reservoir Properties. *Mar. Pet. Geology.* 67, 154–169. doi:10.1016/j.marpetgeo.2015.04.015

Ribeiro, R. C., Correia, J. C. G., and Seidl, P. R. (2009). The Influence of Different Minerals on the Mechanical Resistance of Asphalt Mixtures. *J. Pet. Sci. Eng.* 65 (3-4), 171–174. doi:10.1016/j.petrol.2008.12.025

Ritter, U. (2003). Solubility of Petroleum Compounds in Kerogen. *Org. Geochem.* 34 (3), 319–326. doi:10.1016/S0146-6380(02)00245-0

Romero-Sarmiento, M.-F. (2019). A Quick Analytical Approach to Estimate Both Free Versus Sorbed Hydrocarbon Contents in Liquid-Rich Source Rocks. *AAPG Bull.* 103, 2031–2043. doi:10.1306/02151918152

Sandvik, E. I., Young, W. A., and Curry, D. J. (1992). Expulsion from Hydrocarbon Sources: The Role of Organic Absorption. *Org. Geochem.* 19 (1-3), 77–87. doi:10.1016/0146-6380(92)90028-V

Scheeder, G., Weniger, P., and Blumenberg, M. (2020). Geochemical Implications from Direct Rock-Eval Pyrolysis of Petroleum. *Org. Geochem.* 146, 104051. doi:10.1016/j.orggeochem.2020.104051

Shao, D. Y., Zhang, T. W., Ko, L. T., Li, Y. F., Yan, J. P., Zhang, L. L., et al. (2020). Experimental Investigation of Oil Generation, Retention, and Expulsion Within Type II Kerogen-Dominated Marine Shales: Insights from Gold-Tube Nonhydrous Pyrolysis of Barnett and Woodford Shales Using Miniature Core Plugs. *Int. J. Coal Geology.* 217, 103337. doi:10.1016/j.coal.2019.103337

Soeder, D. J., and Borglum, S. J. (2020). "Part II the Future of Fossil Fuels," in *The Fossil Fuel Revolution: Shale Gas and Tight Oil*. Editors D. J. Soeder and S. J. Borglum (New York, NY: Elsevier), 173–174. doi:10.1016/B978-0-12-815397-0.02002-4

Soeder, D. J., and Borglum, S. J. (2019). "Unconventional Tight Oil and Shale Gas Resources," in *The Fossil Fuel Revolution: Shale Gas and Tight Oil*. Editors

D. J. Soeder and S. J. Borglum (New York, NY: Elsevier), 31–61. doi:10.1016/B978-0-12-815397-0.00003-3

Solarin, S. A. (2020). The Effects of Shale Oil Production, Capital and Labour on Economic Growth in the United States: A Maximum Likelihood Analysis of the Resource Curse Hypothesis. *Resour. Pol.* 68, 101799. doi:10.1016/j.resourpol.2020.101799

Song, D. J., Wang, X. Q., Tuo, J. C., Wu, C. J., Zhang, M. F., Su, L., et al. (2021a). A Comprehensive Study on the Impacts of Rock Fabric on Hydrocarbon Generation and Pore Structure Evolution of Shale Under Semi-confined Condition. *Mar. Pet. Geology.* 124, 104830. doi:10.1016/j.marpetgeo.2020.104830

Song, D. J., Wang, X. Q., Wu, C. J., Meng, S. W., Zhang, M. F., Li, H. D., et al. (2021b). Petroleum Generation, Retention, and Expulsion in Lacustrine Shales Using an Artificial thermal Maturation Approach: Implications for the Iin-Ssitu Conversion of Shale Oil. *Energy Fuels* 35 (1), 358–373. doi:10.1021/acs.energyfuels.0c03045

Song, L. P., Xue, H. T., Lu, S. F., and Tian, S. S. (2015). The Research Progress on the Occurrence Mechanism of Detained Hydrocarbon. *Acta Geologica Sinica - English Edition* 89 (S1), 164–165. doi:10.1111/1755-6724.12303_6

Song, M. S., Liu, H. M., Wang, Y., and Liu, Y. L. (2020). Enrichment Rules and Exploration Practices of Paleogene Shale Oil in Jiyang Depression, Bohai Bay Basin, China. *Pet. Exploration Develop.* 47 (02), 242–253. doi:10.1016/S1876-3804(20)60043-X

Song, Y.-Q., and Kausik, R. (2019). NMR Application in Unconventional Shale Reservoirs - A New Porous Media Research Frontier. *Prog. Nucl. Magn. Reson. Spectrosc.* 112-113, 17–33. doi:10.1016/j.pnmrs.2019.03.002

Spigolon, A. L. D., Lewan, M. D., de Barros Penteado, H. L., Coutinho, L. F. C., and Mendonça Filho, J. G. (2015). Evaluation of the Petroleum Composition and Quality with Increasing thermal Maturity as Simulated by Hydrous Pyrolysis: A Case Study Using a Brazilian Source Rock with Type I Kerogen. *Org. Geochem.* 83-84, 27–53. doi:10.1016/j.orggeochem.2015.03.001

Stainforth, J. G. (2009). Practical Kinetic Modeling of Petroleum Generation and Expulsion. *Mar. Pet. Geology.* 26 (4), 552–572. doi:10.1016/j.marpetgeo.2009.01.006

Stockhausen, M., Galimberti, R., Elias, R., Di Paolo, L., and Schwark, L. (2021). Expulsinator Assessment of Oil/Gas Generation and Expulsion Characteristics of Different Source Rocks. *Mar. Pet. Geology.* 129, 105057. doi:10.1016/j.marpetgeo.2021.105057

Su, K. M., Lu, J. G., Zhang, H. X., Chen, S. J., Li, Y., Xiao, Z. L., et al. (2020). Quantitative Study on Hydrocarbon Expulsion Mechanism Based on Micro-fracture. *Geosci. Front.* 11 (6), 1901–1913. doi:10.1016/j.gsf.2020.05.013

Su, S. Y., Jiang, Z. X., Shan, X. L., Ning, C. X., Zhu, Y. F., Wang, X. Y., et al. (2019). Effect of Lithofacies on Shale Reservoir and Hydrocarbon Bearing Capacity in the Shahejie Formation, Zhanhua Sag, Eastern China. *J. Pet. Sci. Eng.* 174, 1303–1308. doi:10.1016/j.petrol.2018.11.048

Su, S. Y., Jiang, Z. X., Shan, X. L., Zhang, C. W., Zou, Q. T., Li, Z., et al. (2018). The Effects of Shale Pore Structure and Mineral Components on Shale Oil Accumulation in the Zhanhua Sag, Jiyang Depression, Bohai Bay Basin, China. *J. Pet. Sci. Eng.* 165, 365–374. doi:10.1016/j.petrol.2018.02.030

Sun, J., Xiao, X. M., Cheng, P., and Tian, H. (2019). Formation and Evolution of Nanopores in Shales and its Impact on Retained Oil During Oil Generation and Expulsion Based on Pyrolysis Experiments. *J. Pet. Sci. Eng.* 176, 509–520. doi:10.1016/j.petrol.2019.01.071

Sun, J., Xiao, X. M., Cheng, P., Wang, M., and Tian, H. (2021). The Relationship Between Oil Generation, Expulsion and Retention of Lacustrine Shales: Based on Pyrolysis Simulation Experiments. *J. Pet. Sci. Eng.* 196, 107625. doi:10.1016/j.petrol.2020.107625

Sun, L. D., Liu, H., He, W. Y., Li, G. X., Zhang, S. C., Zhu, R. K., et al. (2021). An Analysis of Major Scientific Problems and Research Paths of Gulong Shale Oil in Daqing Oilfield, NE China. *Pet. Exploration Develop.* 48 (3), 527–540. doi:10.1016/S1876-3804(21)60043-5

Sweeney, J. J., and Burnham, A. K. (1990). Evaluation of a Simple Model of Vitrinite Reflectance Based on Chemical Kinetics. *AAPG Bull.* 74 (10), 1559–1570. doi:10.1306/0C9B251F-1710-11D7-8645000102C1865D

Tian, S. S., Erastova, V., Lu, S. F., Greenwell, H. C., Underwood, T. R., Xue, H. T., et al. (2018). Understanding Model Crude Oil Component Interactions on Kaolinite Silicate and Aluminol Surfaces: Toward Improved Understanding of Shale Oil Recovery. *Energy Fuels* 32 (2), 1155–1165. doi:10.1021/acs.energyfuels.7b02763

Tian, S. S., Liu, B., Fu, X. F., Zeng, F., Chi, Y. A., Wu, T., et al. (2020). *A Shale Oil Detection Method and System Based on Occurrence States*. Heilongjiang, China (in Chinese).

Tian, S. S., Xue, H. T., Lu, S. F., and Chen, G. H. (2014). "Discussion on the Mechanism of Different Types of Kerogen Remaining Oil and Gas," in *2014 Annual Meeting of Chinese Geoscience Union* (Beijing: Annual Meeting of Chinese Geoscience Union), 2509–2512. (in Chinese)

Tian, S. S., Xue, H. T., Lu, S. F., Zeng, F., Xue, Q. Z., Chen, G. H., et al. (2017). Molecular Simulation of Oil Mixture Adsorption Character in Shale System. *j nanosci nanotechnol* 17 (9), 6198–6209. doi:10.1166/jnn.2017.14487

Tissot, B. P., and Welte, D. H. (1984). "From Kerogen to Petroleum," in *Petroleum Formation and Occurrence* (Berlin: Springer-Verlag), 160–198. doi:10.1007/978-3-642-87813-8_10

US Energy Information Administration (2021). *US Crude Oil and Natural Gas Proved Reserves, Year-End 2019*. Washington, DC: U.S. Department of Energy.

US Energy Information Administration (2015). *World Shale Resource Assessments*. Washington, DC: U.S. Department of Energy.

Wang, B. Y., Liu, B., Sun, G. X., Bai, L. H., Chi, Y. A., Liu, Q., et al. (2021). Evaluation of the Shale Oil Reservoir and the Oil Enrichment Model for the First Member of the Lucaogou Formation, Western Jimusaer Depression, Junggar Basin, NW China. *ACS Omega* 6 (18), 12081–12098. doi:10.1021/acsomega.1c00756

Wang, E. Z., Feng, Y., Liu, G. Y., Chen, S. R., Wu, Z. Y., and Li, C. R. (2021). Hydrocarbon Source Potential Evaluation Insight into Source Rocks-A Case Study of the First Member of the Paleogene Shahejie Formation, Nanpu Sag, NE China. *Energ. Rep.* 7, 32–42. doi:10.1016/j.egyr.2020.11.099

Wang, E. Z., Liu, G. Y., Pang, X. Q., Li, C. Q., Zhao, Z. F., Feng, Y., et al. (2020). An Improved Hydrocarbon Generation Potential Method for Quantifying Hydrocarbon Generation and Expulsion Characteristics with Application Example of Paleogene Shahejie Formation, Nanpu Sag, Bohai Bay Basin. *Mar. Pet. Geology.* 112, 104106. doi:10.1016/j.marpetgeo.2019.104106

Wang, H., Wang, X. Q., Jin, X., and Cao, D. P. (2016). Molecular Dynamics Simulation of Diffusion of Shale Oils in Montmorillonite. *J. Phys. Chem. C* 120 (16), 8986–8991. doi:10.1021/acs.jpcc.6b01660

Wang, K., Zha, M., and Qu, J. X. (2005). Quantitative Calculation of Hydrocarbon-Generation and Hydrocarbon-Expulsion Amounts in Consideration of Source Rock Heterogeneity. *Acta Petrolei Sinica* (03), 44–47. (in Chinese with English Abstract).

Wang, M., Guo, Z. Q., Jiao, C. X., Lu, S. F., Li, J. B., Xue, H. T., et al. (2019a). Exploration Progress and Geochemical Features of Lacustrine Shale Oils in China. *J. Pet. Sci. Eng.* 178, 975–986. doi:10.1016/j.petrol.2019.04.029

Wang, M., Lu, S. F., Dong, Q., Xue, H. T., and Huang, L. M. (2011). Comparison on Hydrocarbon Generation Kinetic Models. *J. China Univ. Pet. (Edition Nat. Science)* 35 (03), 12–18. (in Chinese with English Abstract).

Wang, M., Lu, S. F., Xue, H. T., Guo, X. B., Chen, G. H., Tian, S. S., et al. (2012). Bulk Pyrolysis and Chemical Kinetic Characteristics of Om Related to the Occurrence of Immature-Low Mature Oils. *Energy Exploration & Exploitation* 30 (1), 71–88. doi:10.1260/0144-5987.30.1.71

Wang, M., Ma, R., Li, J. B., Lu, S. F., Li, C. M., Guo, Z. Q., et al. (2019b). Occurrence Mechanism of Lacustrine Shale Oil in the Paleogene Shahejie Formation of Jiyang Depression, Bohai Bay Basin, China. *Pet. Exploration Develop.* 46 (4), 833–846. doi:10.1016/S1876-3804(19)60242-9

Wang, M., Tian, S. S., Chen, G. H., Xue, H. T., Huang, A. H., and Wang, W. G. (2014). Correction Method of Light Hydrocarbons Losing and Heavy Hydrocarbon Handling for Residual Hydrocarbon (S1) from Shale. *Acta Geologica Sinica - English Edition* 88 (06), 1792–1797. doi:10.1111/1755-6724.12345

Wang, M., Wilkins, R. W. T., Song, G., Zhang, L., Xu, X., Li, Z., et al. (2015). Geochemical and Geological Characteristics of the Es3L Lacustrine Shale in the Bonan Sag, Bohai Bay Basin, China. *Int. J. Coal Geology.* 138, 16–29. doi:10.1016/j.coal.2014.12.007

Wang, S., Feng, Q. H., Javadpour, F., Xia, T., and Li, Z. (2015a). Oil Adsorption in Shale Nanopores and its Effect on Recoverable Oil-In-Place. *Int. J. Coal Geology.* 147-148, 9–24. doi:10.1016/j.coal.2015.06.002

Wang, S., Feng, Q. H., Zha, M., Lu, S. F., Qin, Y., Xia, T., et al. (2015b). Molecular Dynamics Simulation of Liquid Alkane Occurrence State in Pores and Slits of Shale Organic Matter. *Pet. Exploration Develop.* 42 (6), 844–851. doi:10.1016/S1876-3804(15)30081-1

Wang, Y., Wang, X. J., Song, G. Q., Liu, H. M., Zhu, D. S., Zhu, D. Y., et al. (2016). Genetic Connection Between Mud Shale Lithofacies and Shale Oil Enrichment in Jiyang Depression, Bohai Bay Basin. *Pet. Exploration Develop.* 43 (5), 759–768. doi:10.1016/S1876-3804(16)30091-X

Wei, Z., Zou, Y.-R., Cai, Y., Wang, L., Luo, X., and Peng, P. A. (2012). Kinetics of Oil Group-type Generation and Expulsion: An Integrated Application to Dongying Depression, Bohai Bay Basin, China. *Org. Geochem.* 52, 1–12. doi:10.1016/j.orggeochem.2012.08.006

Wu, T., Pan, Z. J., Liu, B., Connell, L. D., Sander, R., and Fu, X. F. (2021). Laboratory Characterization of Shale Oil Storage Behavior: A Comprehensive Review. *Energy Fuels* 35 (9), 7305–7318. doi:10.1021/acs.energyfuels.0c04082

Xi, K. L., Li, K., Cao, Y. C., Lin, M. R., Niu, X. B., Zhu, R. K., et al. (2020). Laminae Combination and Shale Oil Enrichment Patterns of Chang 73 Sub-member Organic-Rich Shales in the Triassic Yanchang Formation, Ordos Basin, NW China. *Pet. Exploration Develop.* 47 (06), 1342–1353. doi:10.1016/S1876-3804(20)60142-8

Xiao, L. H., Meng, Y. L., Zhang, L. X., Wei, A. J., Li, J., Zhang, W. C., et al. (2005). Vitrinite Reflectance Modeling in the Over-pressured Formations. *Pet. Explor. Dev.* (01), 14–17. (in Chinese with English Abstract).

Xie, X. M., Krooss, B. M., Littke, R., Amann-Hildenbrand, A., Li, M. W., Li, Z. M., et al. (2019). Accessibility and Mobility of Hydrocarbons in Lacustrine Shale: Solvent Flow-Through Extraction Experiments on Eocene Oil Shales from Bohai Bay Basin, Eastern China. *Org. Geochem.* 127, 23–36. doi:10.1016/j.orggeochem.2018.11.006

Xu, Z. J., Liu, L. F., Liu, B. J. M., Wang, T. G., Zhang, Z. H., Wu, K. J., et al. (2019). Geochemical Characteristics of the Triassic Chang 7 Lacustrine Source Rocks, Ordos Basin, China: Implications for Paleoenvironment, Petroleum Potential and Tight Oil Occurrence. *J. Asian Earth Sci.* 178, 112–138. doi:10.1016/j.jseaes.2018.03.005

Xue, H. T., Tian, S. S., Lu, S. F., Zhang, W. H., Du, T. T., and Mu, G. D. (2015). Selection and Verification of Key Parameters in the Quantitative Evaluation of Shale Oil: A Case Study at the Qingshankou Formation, Northern Songliao Basin. *Bull. Mineralogy. Petrol. Geochem.* 34 (01), 70–78. doi:10.3969/j.issn.1007-2802.2015.01.008 (in Chinese with English Abstract).

Yang, L., and Jin, Z. J. (2019). Global Shale Oil Development and Prospects. *China Pet. Exploration* 24 (05), 553–559. doi:10.3969/j.issn.1672-7703.2019.05.002 (in Chinese with English Abstract).

Yang, Z., and Zou, C. N. (2019). "Exploring Petroleum inside Source Kitchen": Connotation and Prospects of Source Rock Oil and Gas. *Pet. Exploration Develop.* 46 (01), 181–193. doi:10.1016/S1876-3804(19)30018-7

Yang, Z., Zou, C. N., Wu, S. T., Lin, S. H., Pan, S. Q., Niu, X. B., et al. (2019). Formation, Distribution and Resource Potential of the "Sweet Areas (Sections)" of Continental Shale Oil in China. *Mar. Pet. Geol.* 102, 48–60. doi:10.1016/j.marpetgeo.2018.11.049

Yusupova, T. N., Romanova, U. G., Gorbachuk, V. V., Muslimov, R. K., and Romanov, G. V. (2002). Estimation of the Adsorption Capacity of Oil-Bearing Rocks: A Method and its Prospects. *J. Pet. Sci. Eng.* 33 (1–3), 173–183. doi:10.1016/S0920-4105(01)00184-X

Zeng, X., Cai, J. G., Dong, Z., Wang, X. J., and Hao, Y. Q. (2017). Sedimentary Characteristics and Hydrocarbon Generation Potential of Mudstone and Shale: A Case Study of Middle Submember of Member 3 and Upper Submember of Member 4 in Shahejie Formation in Dongying Sag. *Acta Petrolei Sinica* 38 (01), 31–43. doi:10.7623/syxb201701004 (in Chinese with English Abstract).

Zhang, D. W., Wang, L. H., Su, L., Wu, Y. D., Sun, R., Wu, C. J., et al. (2020). The Chemical Kinetics of the Semi-open Hydrous Pyrolysis System: Time Series Analysis of Lithostatic Pressure and Fluid Pressure. *Int. J. Coal Geology.* 220, 103418. doi:10.1016/j.coal.2020.103418

Zhang, H., Huang, H. P., Li, Z., and Liu, M. (2020). Comparative Study Between Sequential Solvent-Extraction and Multiple Isothermal Stages Pyrolysis: A Case Study on Eocene Shahejie Formation Shales, Dongying Depression, East China. *Fuel* 263, 116591. doi:10.1016/j.fuel.2019.116591

Zhang, L. Y., Xu, X. Y., Liu, Q., Kong, X. X., and Zhang, S. C. (2011). Hydrocarbon Formation and Accumulation of the Deep Paleogene of the Jiyang Depression, Shengli Oilfield. *Pet. Exploration Develop.* 38 (5), 530–537. doi:10.1016/S1876-3804(11)60053-0

Zhang, L. Y., Bao, S. Y., Li, J. Y., Li, Z., Zhu, R. F., Zhang, L., et al. (2015). Hydrocarbon and Crude Oil Adsorption Abilities of Minerals and Kerogens in Lacustrine Shales. *Pet. Geology. Exp.* 37 (6), 776–780. doi:10.11781/sysydz201506776 (in Chinese with English Abstract).

Zhang, P. F., Lu, S. F., Li, J. Q., and Chang, X. C. (2020). 1D and 2D Nuclear Magnetic Resonance (NMR) Relaxation Behaviors of Protons in clay, Kerogen and Oil-Bearing Shale Rocks. *Mar. Pet. Geology.* 114, 104210. doi:10.1016/j.marpetgeo.2019.104210

Zhang, P. L., Misch, D., Hu, F., Kostoglou, N., Sachsenhofer, R. F., Liu, Z. J., et al. (2021). Porosity Evolution in Organic Matter-Rich Shales (Qingshankou Fm.; Songliao Basin, NE China): Implications for Shale Oil Retention. *Mar. Pet. Geology.* 130, 105139. doi:10.1016/j.marpetgeo.2021.105139

Zhang, P. Y., Jiang, F. J., Zhu, C. X., Huang, R. D., Hu, T., Xu, T. W., et al. (2021). Gas Generation Potential and Characteristics of Oil-Prone Shale in the Saline Lacustrine Rifting Basins: A Case Study of the Dongpu Depression, Bohai Bay Basin. *Energy Fuels* 35, 2192–2208. doi:10.1021/acs.energyfuels.0c03965

Zhang, S. J., Li, Y. H., and Pu, H. (2020). Studies of the Storage and Transport of Water and Oil in Organic-Rich Shale Using Vacuum Imbibition Method. *Fuel* 266, 117096. doi:10.1016/j.fuel.2020.117096

Zhang, S., Liu, H. M., Song, G. Q., Wang, Y. S., Chen, S. Y., and Zhang, S. P. (2016). Genesis and Control Factors of Shale Oil Reserving Space in Dongying Sag. *Acta Petrolei Sinica* 37 (12), 1495–1507. doi:10.7623/syxb201612005 (in Chinese with English Abstract).

Zhang, W., Feng, Q. H., Wang, S., and Xing, X. D. (2019). Oil Diffusion in Shale Nanopores: Insight of Molecular Dynamics Simulation. *J. Mol. Liquids* 290, 111183. doi:10.1016/j.molliq.2019.111183

Zhang, W. Z., Yang, H., Li, J. F., and Ma, J. (2006). Leading Effect of High-Class Source Rock of Chang 7 in Ordos basin on Enrichment of Low Permeability Oil-Gas Accumulation-Hydrocarbon Generation and Expulsion Mechanism. *Pet. Explor. Dev.* 33 (3), 289–293. (in Chinese with English Abstract).

Zhao, W. Z., Hu, S. Y., and Hou, L. H. (2018). Connotation and Strategic Role of In-Situ Conversion Processing of Shale Oil Underground in the Onshore China. *Pet. Exploration Develop.* 45 (4), 563–572. doi:10.1016/S1876-3804(18)30063-6

Zhao, W. Z., Hu, S. Y., Hou, L. H., Yang, T., Li, X., Guo, B. C., et al. (2020). Types and Resource Potential of Continental Shale Oil in China and its Boundary with Tight Oil. *Pet. Exploration Develop.* 47 (1), 1–11. doi:10.1016/S1876-3804(20)60001-5

Zhao, W. Z., Zhang, B., Wang, X. M., Wu, S. T., Zhang, S. C., Liu, W., et al. (2021). Differences in Source Kitchens for Lacustrine In-Source and Out-Source Hydrocarbon Accumulations Onshore China. *Pet. Exploration Develop.* 48 (03), 464–475. doi:10.1016/s1876-3804(21)60044-7

Zhao, X. Y., Sang, Q., Li, Y. J., Shi, L. Y., Liu, H. M., and Dong, M. Z. (2021). Mobilization of Oil in Organic Matter and its Contribution to Oil Production During Primary Production in Shale. *Fuel* 287, 119449. doi:10.1016/j.fuel.2020.119449

Zhao, X. Z., Zhou, L. H., Pu, X. G., Jin, F. M., Shi, Z. N., Han, W. Z., et al. (2020). Formation Conditions and Enrichment Model of Retained Petroleum in Lacustrine Shale: A Case Study of the Paleogene in Huanghua Depression, Bohai Bay Basin, China. *Pet. Exploration Develop.* 47 (05), 916–930. doi:10.1016/S1876-3804(20)60106-9

Zhao, X. Z., Pu, X. G., Zhou, L. H., Jin, F. M., Han, H. M., Shi, Z. N., et al. (2021). Enrichment Theory, Exploration Technology and Prospects of Shale Oil in Lacustrine Facies Zone of Deep Basin: A Case Study of the Paleogene in Huanghua depression, Bohai Bay Basin. *Acta Petrolei Sinica* 42 (02), 143–162. doi:10.7623/syxb202102001 (in Chinese with English Abstract).

Zhao, X. Z., Zhou, L. H., Pu, X. G., Jin, F. M., Shi, Z. N., Xiao, D. Q., et al. (2019). Favorable Formation Conditions and Enrichment Characteristics of Lacustrine Facies Shale Oil in Faulted Lake basin: A Case Study of Member 2 of Kongdian Formation in Cangdong Sag,Bohai Bay Basin. *Acta Petrolei Sinica* 40 (09), 1013–1029. doi:10.7623/syxb201909001 (in Chinese with English Abstract).

Zhu, R. F., Zhang, L. Y., Li, J. Y., Liu, Q., Li, Z., Wang, R., et al. (2015). Quantitative Evaluation of Residual Liquid Hydrocarbons in Shale. *Acta Petrolei Sinica* 36 (01), 13–18. doi:10.7623/syxb201501002 (in Chinese with English Abstract).

Zhu, X. J., and Cai, J. G. (2012). Progress and Significance of Research on Relation Between Specific Surface Area and Organic Matter in Argillaceous Source Rocks. *Oil Gas Geology.* 33 (03), 375–384. (in Chinese with English Abstract).

Zink, K.-G., Scheeder, G., Stueck, H. L., Biermann, S., and Blumenberg, M. (2016). Total Shale Oil Inventory from an Extended Rock-Eval Approach on Non-extracted and Extracted Source Rocks from Germany. *Int. J. Coal Geology.* 163, 186–194. doi:10.1016/j.coal.2016.06.023

Zou, C. N., Jin, X., Zhu, R. K., Gong, G. M., Sun, L., Dai, J. X., et al. (2015). Do Shale Pore Throats Have a Threshold Diameter for Oil Storage? *Sci. Rep.* 5, 13619. doi:10.1038/srep13619

Zou, C. N., Ding, Y. H., Lu, Y. J., Liu, G. X., Chen, J. J., Wang, X., et al. (2017). Theory, Technology and Practice of "Man-made Reservoirs". *Pet. Explor. Dev.* 44 (1), 144–154. doi:10.1016/s1876-3804(17)30019-8

Zou, C. N., Pan, S. Q., Horsfield, B., Yang, Z., Hao, S. Y., Liu, E. T., et al. (2019a). Oil Retention and Intrasource Migration in the Organic-Rich Lacustrine Chang 7 Shale of the Upper Triassic Yanchang Formation, Ordos Basin, central China. *AAPG Bull.* 103 (11), 2627–2663. doi:10.1306/01301917052

Zou, C. N., Yang, Z., Cui, J. W., Zhu, R. K., Hou, L. H., Tao, S. Z., et al. (2013). Formation Mechanism, Geological Characteristics and Development Strategy of Nonmarine Shale Oil in China. *Pet. Exploration Develop.* 40 (1), 15–27. doi:10.1016/S1876-3804(13)60002-6

Zou, C. N., Zhu, R. K., Chen, Z.-Q., Ogg, J. G., Wu, S. T., Dong, D. Z., et al. (2019b). Organic-matter-rich Shales of China. *Earth-Science Rev.* 189, 51–78. doi:10.1016/j.earscirev.2018.12.002

Zou, Y.-R., Sun, J.-N., Li, Z., Xu, X., Li, M., and Peng, P. A. (2018). Evaluating Shale Oil in the Dongying Depression, Bohai Bay Basin, China, Using the Oversaturation Zone Method. *J. Pet. Sci. Eng.* 161, 291–301. doi:10.1016/j.petrol.2017.11.059